

# 14-3-3 $\sigma$ /Stratifin and p21 limit AKT-related malignant progression in skin carcinogenesis following MDM2-associated p53 loss

Carol M. McMenemy<sup>1</sup> | Dajiang Guo<sup>1</sup> | Jean A. Quinn<sup>2</sup> | David A. Greenhalgh<sup>1</sup> 

<sup>1</sup>Section of Dermatology and Molecular Carcinogenesis, School of Medicine, Dentistry and Nursing, College of Medical, Veterinary and Life Sciences, Glasgow University, Glasgow, Scotland

<sup>2</sup>Wolfson Wohl Cancer Research Centre, Institute of Cancer Sciences, College of Medical, Veterinary and Life Sciences, University of Glasgow, Glasgow, Scotland

## Correspondence

David A. Greenhalgh, Section of Dermatology and Molecular Carcinogenesis, School of Medicine, Dentistry and Nursing, College of Medical, Veterinary and Life Sciences, Glasgow University, Glasgow G31 2ER, Scotland.

Email: [david.greenhalgh@glasgow.ac.uk](mailto:david.greenhalgh@glasgow.ac.uk)

## Present addresses

Carol M. McMenemy, Paterson Laboratories, Cancer Research UK Manchester Institute, The University of Manchester, Manchester, UK.

Dajiang Guo, Department of Medicine, Division of Hematology/Oncology, Weill Cornell Medicine, New York, New York, USA.

## Funding information

Scott Endowment Fund for Dermatology; GU M.Res Research Program in Cancer Sciences; SFC/MRC M.Res in Integrative Mammalian Biology, Glasgow University; Wellcome Biomedical vacation scholarship, Grant/Award Number: UNS22162

## Abstract

To study mechanisms driving/inhibiting skin carcinogenesis, stage-specific expression of 14-3-3 $\sigma$  (Stratifin) was analyzed in skin carcinogenesis driven by activated *ras*<sup>Ha</sup>/*fos* expression (*HK1.ras/fos*) and ablation of *PTEN*-mediated AKT regulation (*K14.creP/Δ5PTEN*<sup>flx/flx</sup>). Consistent with 14-3-3 $\sigma$  roles in epidermal differentiation, *HK1.ras* hyperplasia and papillomas displayed elevated 14-3-3 $\sigma$  expression in supra-basal keratinocytes, paralleled by supra-basal p-MDM2<sup>166</sup> activation and sporadic p-AKT<sup>473</sup> expression. In bi-genic *HK1.fos/Δ5PTEN*<sup>flx/flx</sup> hyperplasia, basal-layer 14-3-3 $\sigma$  expression appeared, and alongside p53/p21, was associated with keratinocyte differentiation and keratoacanthoma etiology. Tri-genic *HK1.ras/fos-Δ5PTEN*<sup>flx/flx</sup> hyperplasia/papillomas initially displayed increased basal-layer 14-3-3 $\sigma$ , suggesting attempts to maintain supra-basal p-MDM2<sup>166</sup> and protect basal-layer p53. However, *HK1.ras/fos-Δ5PTEN*<sup>flx/flx</sup> papillomas exhibited increasing basal-layer p-MDM2<sup>166</sup> activation that reduced p53, which coincided with malignant conversion. Despite p53 loss, 14-3-3 $\sigma$  expression persisted in well-differentiated squamous cell carcinomas (wdSCCs) and alongside elevated p21, limited malignant progression via inhibiting p-AKT<sup>473</sup> expression; until 14-3-3 $\sigma$ /p21 loss facilitated progression to aggressive SCC exhibiting uniform p-AKT<sup>473</sup>. Analysis of TPA-promoted *HK1.ras-Δ5PTEN*<sup>flx/flx</sup> mouse skin, demonstrated early loss of 14-3-3 $\sigma$ /p53/p21 in hyperplasia and papillomas, with increased p-MDM2<sup>166</sup>/p-AKT<sup>473</sup> that resulted in rapid malignant conversion and progression to poorly differentiated SCC. In 2D/3D cultures, membranous 14-3-3 $\sigma$  expression observed in normal HaCaT and SP1<sup>ras61</sup> papilloma keratinocytes was unexpectedly detected in malignant T52<sup>ras61/v-fos</sup> SCC cells cultured in monolayers, but not invasive 3D-cells. Collectively, these data suggest 14-3-3 $\sigma$ /Stratifin exerts suppressive roles in papillomatogenesis via MDM2/p53-dependent

**Abbreviations:**  $\Delta 5PTEN$ <sup>flx/flx</sup>, transgenic mice homozygous for lox-P flanked exon 5 *PTEN*; *HK1.fos*, transgenic mice expressing *FBJ/R v-fos* from a truncated human keratin K1 promoter; *HK1.fos-Δ5PTEN*<sup>flx/flx</sup>, bi-genic progeny of mating *HK1.fos* and *K14.creP-Δ5PTEN* mice; *HK1.ras*, transgenic mice expressing *v-ras*<sup>Ha</sup> exclusively in the epidermis employing a truncated human keratin K1 promoter; *HK1.ras/fos-Δ5PTEN*<sup>flx/flx</sup>, tri-genic progeny of mating *HK1.ras*, *HK1.fos* and *K14.creP-Δ5PTEN* mice; *K14.creP*, transgenic mice expressing RU486 responsive cre recombinase from a keratin K14 promoter; *K14.cre-Δ5PTEN*<sup>flx/flx</sup>, bi-genic progeny of mating *K14.creP* and  $\Delta 5PTEN$  mice; KA, keratoacanthoma; SCC, squamous cell carcinoma.

This is an open access article under the terms of the [Creative Commons Attribution](https://creativecommons.org/licenses/by/4.0/) License, which permits use, distribution and reproduction in any medium, provided the original work is properly cited.

© 2024 The Author(s). *Molecular Carcinogenesis* published by Wiley Periodicals LLC.

mechanisms; while persistent p53-independent expression in early wdSCC may involve p21-mediated AKT1 inhibition to limit malignant progression.

#### KEYWORDS

fos, keratoacanthoma, organotypic culture, PTEN, ras, skin carcinogenesis, TPA promotion, transgenic mouse

## 1 | INTRODUCTION

The 14-3-3 family of phospho-proteins modulate an extensive and wide variety of pathways ranging from metabolism and autophagy; through cell cycle regulation, proliferation, and apoptosis; to cell motility, spatial awareness, and differentiation.<sup>1–5</sup> In carcinogenesis, deregulated 14-3-3 $\sigma$  is the most common isoform,<sup>6–8</sup> however, given the plethora of pathways and their complex interactions,<sup>1–5</sup> 14-3-3 $\sigma$  causality remains elusive; exhibiting both tumor suppressive and oncogenic roles dependent upon context. Loss of tumor suppressive functions, via promoter hypermethylation rather than mutation/deletion,<sup>6,9</sup> appear in diverse tumors including receptor-positive breast cancers,<sup>8</sup> liver,<sup>9</sup> small cell and neuroendocrine lung cancers<sup>10</sup> and correlate with poor prognosis. In contrast, promoter hypo-methylation giving 14-3-3 $\sigma$  overexpression appears in lung adenocarcinoma,<sup>11</sup> nonsmall cell lung cancer,<sup>12</sup> and colorectal cancers<sup>13</sup>; with overexpression of the secreted form appearing in liver cancer.<sup>14</sup> 14-3-3 $\sigma$  positivity was more common in triple-negative versus receptor-positive breast cancers and despite acting as an inhibitory MDM2 chaperone,<sup>3,4</sup> resultant p53 increase conferred poorer prognosis.<sup>8</sup> Gastrointestinal cancers further highlight contrasting p53 interactions, as some studies show independent 14-3-3 $\sigma$ /p53 expression,<sup>15</sup> others showed strong correlation with p53 mutations; for example, in colonic tumors; yet survival rates were associated with 14-3-3 $\sigma$  loss in tumors wild type for p53.<sup>16</sup>

In epidermis, 14-3-3 $\sigma$  is associated with multiple roles in differentiation, spatial awareness/cellular orientation, and motility of both interfollicular and follicular keratinocytes.<sup>5,17–19</sup> In human skin carcinogenesis, while 14-3-3 $\sigma$  was implicated in basal cell carcinoma via classic TSG loss, this study found increased 14-3-3 $\sigma$  expression in squamous cell carcinoma (SCC).<sup>20</sup> This suggests that initial, increased 14-3-3 $\sigma$  protected p53 expression<sup>3,4,21</sup> via MDM2 chaperone/degradation, thus maintaining nuclear p53 levels.<sup>3,4,22</sup> However, if p53 was mutated by UV-B, this mechanism would be counter-productive, resulting in an oncogenic loop of p53 loss-/gain-of-function mutant expression<sup>21</sup> again reflecting contrasting roles in specific tumor contexts.<sup>9–16</sup> Mouse models highlight tumor suppressive roles, as the *Er/Er<sup>+/-</sup>* repeated epilation stain possesses germline 14-3-3 $\sigma$  mutations that result in epidermal hyperplasia, failed follicular differentiation, and susceptibility to SCC.<sup>23,24</sup> Conditional 14-3-3 $\sigma$  knockout co-operated with ErbB2 in mammary carcinogenesis<sup>25</sup>; while in DMBA/TPA carcinogenesis, 14-3-3 $\sigma$  loss resulted in rapid papilloma formation, supporting a promoting role.<sup>26</sup>

To further investigate inhibitory/oncogenic functions, 14-3-3 $\sigma$  expression was investigated in skin carcinogenesis driven by *ras<sup>Ha</sup>/fos*

activation and conditional loss of *PTEN*-mediated AKT inhibition.<sup>27–29</sup> *HK1.ras/fos- $\Delta$ 5PTEN<sup>flx/flx</sup>* mice display papillomatogenesis associated with compensatory p53/p21 that delayed/inhibited malignant conversion or produced benign keratoacanthomas (KAs) (*HK1.fos- $\Delta$ 5PTEN<sup>flx/flx</sup>*).<sup>27–29</sup> Following p53 loss and malignant conversion, *HK1.ras/fos- $\Delta$ 5PTEN<sup>flx/flx</sup>* tumors retained p21 expression, which limited progression to well-differentiated SCC (wdSCC); until p21 loss<sup>29</sup> gave progression to poorly differentiated SCC (pdSCC). This provided an opportunity to investigate stage-specific 14-3-3 $\sigma$  interactions with MDM2 and p53 that inhibit/drive papilloma conversion; while loss of *PTEN*-mediated AKT inhibition investigated links between p21 and 14-3-3 $\sigma$  that may limit malignant progression via AKT inhibition.<sup>30–32</sup>

Key findings demonstrated 14-3-3 $\sigma$  expression increase in hyperplastic and papilloma basal-layers was paralleled by increased p53/p21 expression. Subsequently, reduced 14-3-3 $\sigma$  in papilloma basal-layers was associated with supra-basal-to-basal increases in p-MDM2<sup>166</sup> activation; with corresponding reduction in p53, which contributed to malignant conversion. Further, following p53 loss, persistent 14-3-3 $\sigma$  expression observed in wdSCCs, alongside elevated p21 may limit early-stage malignant progression via inhibition of p-AKT1<sup>473</sup> activation, as 14-3-3 $\sigma$ /p21 loss led to increased p-AKT1<sup>473</sup> and progression to aggressive SCC. Although an oncogenic role for persistent 14-3-3 $\sigma$  cannot be excluded, as also suggested by persistent 14-3-3 $\sigma$  expression in 3D cultures, TPA promotion of *HK1.ras- $\Delta$ 5PTEN<sup>flx</sup>* mice induced rapid transit to pdSCC, associated with early 14-3-3 $\sigma$ /p53/p21 loss and immediate, uniform p-AKT1<sup>473</sup> expression, which collectively support tumor suppressive roles for 14-3-3 $\sigma$  in this model.

## 2 | METHODS

### 2.1 | Transgenic genotypes and induction of tumors

Adult transgenic mice (5–16 weeks old) expressing activated *ras<sup>Ha</sup>* and/or *v-fos* from a human keratin K1-based vector, modified to express in basal- and supra-basal keratinocytes (*HK1.ras/fos*) have been described previously.<sup>33</sup> To explore malignant conversion, *HK1.ras/fos* mice were crossed to mice expressing a keratin K14-driven, RU486-inducible cre fusion protein (*K14.creP<sup>34</sup>*) and mice expressing a *lox-P*-flanked-*PTEN* exon 5 allele ( *$\Delta$ 5PTEN<sup>flx/flx</sup>*).<sup>27–29</sup> *HK1.ras/fos- $\Delta$ 5PTEN<sup>flx/flx</sup>* progeny were genotyped by PCR (see

Supporting Information: Table 1). PTEN function was inactivated (15 per cohort in repeat experiments<sup>27–29</sup>) following 3 topical treatments with 15  $\mu\text{L}$ , 2  $\mu\text{g}/\text{mL}$  RU486 (mifepristone; Sigma) in ethanol; controls (5 per cohort) received ethanol alone; giving an archive of up to 60 RU-486 treated ear tumor and 30 dorsal skin biopsy samples per cohort. Tumors were raised in adult RU486-treated, bi-genic *HK1.ras*- $\Delta 5\text{PTEN}^{\text{flx/flx}}$  mice ( $n = 10$ ) via 2 weekly treatments with 2.5  $\mu\text{g}/50 \mu\text{L}$  acetone TPA (50  $\mu\text{L}$  of  $1.6 \times 10^{-4}$  M TPA; Sigma) with controls ( $n = 5$ ) receiving RU486 and ethanol alone.

As observed previously, individuals from each transgenic cohort produced similar, if not identical phenotypes; for instance, all *HK1.ras* mice exhibit papillomas by 8–10 weeks<sup>27,33</sup> and while *HK1.fos* provides a promotion stimulus,<sup>28</sup> all bi-genic *HK1.ras/fos* mice lack spontaneous malignant conversion.<sup>33</sup> Similarly, bi-genic *HK1.ras/\Delta 5\text{PTEN}^{\text{flx/flx}}* papillomas required TPA promotion to achieve malignancy<sup>27</sup>; while bi-genic *HK1.fos-\Delta 5\text{PTEN}^{\text{flx/flx}}* progeny developed benign KAs, not wdSCC, associated with compensatory p53/p21 expression.<sup>28</sup> Additional  $\text{ras}^{\text{Ha}}$  expression in tri-genic *HK1.ras/fos-\Delta 5\text{PTEN}^{\text{flx/flx}}* progeny led to malignant conversion associated with spontaneous p53 loss, whereas p21 retention limited progression to wdSCC<sup>29</sup> (see Supporting Information: Figures S2 and S7). All experiments adhered to UK Experimental Regulations governing animal experimentation (Licence: P82170325 to DAG). In addition to this licence, Animal Care and Use was approved by Glasgow University Advisory Committee on Genetic Manipulation: Animal Use Committee (GM Center number: 318).

## 2.2 | Histology, immunofluorescence, and immunochemical analysis

Skin biopsies and organotypic rafts were fixed in buffered formalin (24 h at 4°C), embedded in paraffin and stained with haematoxylin and eosin. Differentiation status was assessed via double-label immunofluorescence. A minimum of 15, randomly selected ear tumor/dorsal skin biopsies were analyzed per genotype; and wherever possible, for direct comparison, the data shown in each figure employed serial sections from previously published archival tumor blocks.<sup>27–29</sup> Following antigen retrieval (boil 5 min/10 mM sodium citrate), sections were incubated overnight (4°C) with: rabbit anti-mK1 (BioLegend Cat#905601, RRID: AB2565051; 1:100) employing guinea-pig anti-K14 to delineate epidermis/tumor (Progen Cat#GP-CK14, RRID: AB2920669; 1:200). Expression was visualized with FITC-labeled anti-rabbit IgG (Jackson Labs Cat#711-096-152, RRID: AB2340597; 1:100) or biotinylated-goat anti-guinea pig (Vector Laboratories Cat#BA-7000, RRID: AB2336132; 1:100) and Streptavidin-Texas Red (Vector Laboratories Cat#SA-5006, RRID: AB2336754; 1:400) at room temperature for 60 min. 14-3-3 $\sigma$ /Stratifin analysis employed rabbit anti-14-3-3 $\sigma$ /Stratifin (Thermo-Fisher Cat#PA5-23507, RRID: AB2544623; 1:100) and p-AKT1<sup>s473</sup> activation employed rabbit anti-p-AKT1<sup>s473</sup> (Abcam Cat# ab81283, RRID: AB2224551; 1:100).

For immunohistochemical analysis, following antigen retrieval, sections were incubated overnight (4°C) with rabbit anti-14-3-3 $\sigma$ /Stratifin (1:100); and rabbit anti p-MDM2<sup>166</sup> (Abcam anti-MDM2 phospho-S166; Cat#ab131355, RRID: AB11157309; 1:400). p53 analysis employed Abcam Cat# ab31333, RRID: AB\_776980 (diluted 1:50) and p21 employed Proteintech Cat# #10355-1-AP, RRID: AB\_2077682 (diluted 1:200) which replaced Santa Cruz p53 (sc#393) and p21 (Cat# sc-397) (see Supporting Information: Figure S1). For analysis of 2D chamber cultures, cells were fixed in 10% formalin, washed and incubated overnight (4°C) with rabbit anti-14-3-3 $\sigma$ /Stratifin (1:100). Expression visualized via HRP-conjugated goat anti-rabbit antibodies (Vector Laboratories Cat#PAB21463HRP-1000, RRID: AB2916034; 1:100) at room temp for 60 min followed by DAB+ staining (Dako; Amersham Biosciences).

Photomicrographs employed Axiovision image software (Axiovision Imaging System, RRID: SCR002677; Zeiss Microscopes). Image J was employed to quantitate expression data via double-blind analysis. Typically, 20 areas were measured per inverted, 8-bit tif image (see Supporting Information: Figure S4) and optical density (OD; corrected minus background) results averaged per image. Up to 12 separate tumor images representative of each treated cohort were analyzed (see Supporting Information: Figures S3–S5) and significance determined via two-way ANOVA analysis.

## 2.3 | Cell culture and organotypic tumor invasion modeling

Immortalized human HaCaT keratinocytes (36; RRID: CVCL0038); were provided at passage 35 and used at passages 45–53. DMBA-initiated/TPA promoted,  $\text{ras}^{\text{Ha}}$ -transformed SP1 papilloma cells (RRID: CVCL5785; passage 47–53) and  $\text{ras}^{\text{Ha}}$ /fos transformed T52 carcinoma cells (37; DAG originated; passage 30–36) were cultured in DMEM (w/o  $\text{Ca}^{2+}$ ), supplemented with 10% (chelated) fetal calf serum (FCS) and 0.05 mM calcium (Low  $\text{Ca}^{2+}$ ).<sup>35</sup> C8161 melanoma cells (RRID: CVCL6813; passage number unknown) were cultured in DMEM/10% FCS.

For IHC or IF analysis, cells were plated at 1000 cells per chamber (Millicell EZ SLIDE; Millipore) in Low  $\text{Ca}^{2+}$  media, and 2 days later induced to differentiated by culture in 0.12 mM  $\text{Ca}^{2+}$  media for 48 h<sup>35</sup> and fixed in 10% formalin (Sigma).

Organotypic invasion models<sup>36</sup> were prepared by extracting collagen from rat tail tendons with 0.5 M acetic acid. Typically, 3 mL 10X DMEM/30% FCS was added to 25 mL rat tail collagen (2 mg/mL; 4°C), neutralized with 0.22 M sodium hydroxide (pH 7.2) and dermal fibroblasts ( $7 \times 10^4$  cells/mL) seeded in 2.5 mL neutralized collagen and plated into 35 mm dishes. Collagen rafts formed within 7 days (~1.5 cm diameter) and were placed into 24-well dishes containing 1 mL media and seeded with  $10^4$  cells; employing C8161 melanoma cells (RRID: CVCL6813) as a positive control. Each cell-matrix was cultured for 3 days, transferred to 60 mm dishes containing a submerged grid and 3 days later, cells were raised to the air liquid interface for a further 8–10 days.<sup>36</sup>

### 3 | RESULTS

#### 3.1 | 14-3-3 $\sigma$ expression in differentiating supra-basal keratinocytes becomes elevated in proliferative, basal-layer papillomas

To investigate normal function and roles in papillomatogenesis, 14-3-3 $\sigma$  expression was compared to p53 and p21 status in normal skin and *HK1.ras* hyperplasia/papillomas (Figure 1A–C). In normal epidermis 14-3-3 $\sigma$  was expressed in supra-basal layers,

with occasional expression in proliferative, basal-layer keratinocytes (Figure 1A), paralleled by supra-basal keratin K1 expression, an early marker of differentiation, also expressed in occasional basal-layer keratinocytes on commitment to differentiate (Figure 1A); while p53/p21 were expressed in sporadic cycling keratinocytes (see also Supporting Information: Figure S7). These 14-3-3 $\sigma$ /K1 co-expression data were consistent with roles in epidermal differentiation, while sporadic basal-layer expression suggests 14-3-3 $\sigma$  also regulates keratinocyte commitment to differentiate.

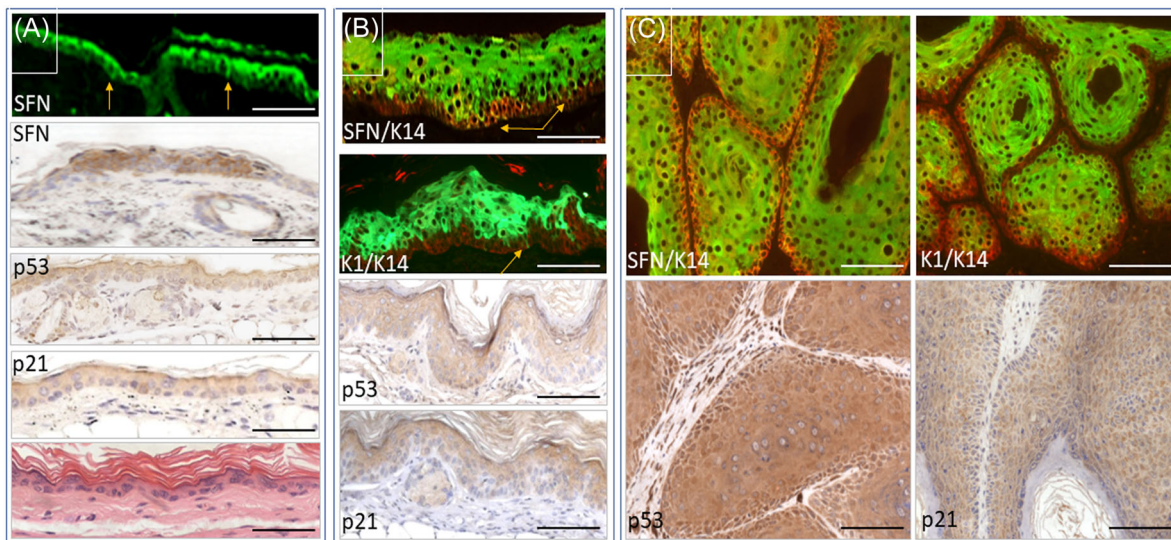


**Fig.1 B & C: 14-3-3s, K1, p53 and p21**

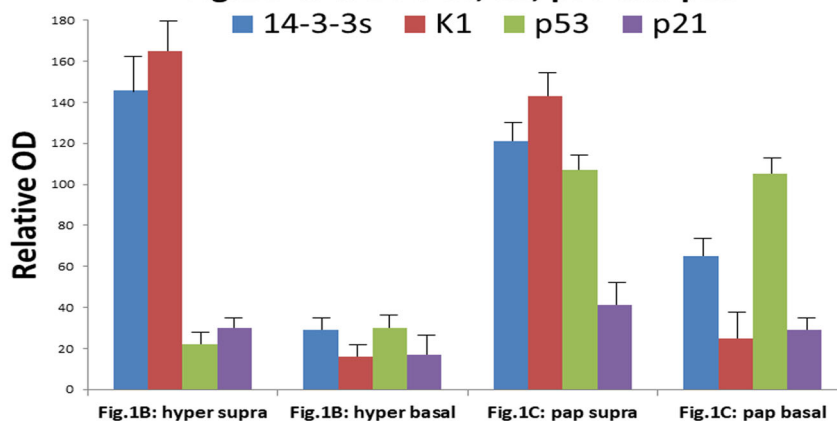


**FIGURE 1** 14-3-3 $\sigma$ , p53 and p21 expression in normal and premalignant phenotypes. (A) Single-label IF/IHC analysis of normal epidermis shows supra-basal 14-3-3 $\sigma$  expression (SFN) with sporadic, expression in (narrow) basal-layer keratinocytes (arrows) committing to differentiate; while cycling basal-layer keratinocytes show low-level p53/p21. Bottom panel: normal histology. (B) IF analysis of *HK1.ras* hyperplasia displays supra-basal 14-3-3 $\sigma$  expression (SFN green), with occasional positive (yellow) differentiating basal-layer keratinocytes (arrows); Keratin K14 (red) indicates basal layer. Keratin K1 (green) and K14 (red) show similar differentiation pattern of supra-basal K1 and basal K14; with narrow, basal-layer keratinocytes committing to differentiate. IHC analysis shows sporadic, low-level p53/p21 expression. (C) *HK1.ras* papillomas show supra-basal 14-3-3 $\sigma$ , with increasing expression in basal-layer keratinocytes (orange); while supra-basal K1 indicates benign tumor. IHC analysis now shows elevated/nuclear p53 in basal layer keratinocytes. Image J quantitation of *HK1.ras* hyperplasia confirms high 14-3-3 $\sigma$ /K1 expression in supra-basal layers; with low expression in basal keratinocytes; alongside low p53/p21. *HK1.ras* papillomas show a similar supra-basal 14-3-3 $\sigma$ /K1 profile but now exhibit increased 14-3-3 $\sigma$  in basal layers paralleled by a fourfold increase in p53 and weaker twofold p21 expression. Bars (A) approximately 25–30  $\mu$ m; (B) approximately 65  $\mu$ m; (C) SFN/K14 & K1/K14 approximately 50  $\mu$ m; p53 approximately 75  $\mu$ m; p21 approximately 100  $\mu$ m.

In *HK1.ras* hyperplasia, a similar supra-basal 14-3-3 $\sigma$  expression profile was observed, alongside occasional positive basal-layer cells as keratinocytes committed to differentiate (paralleled by K1 expression; see Supporting Information: Figure S7); with sporadic p53/p21 expression in cycling cells (Figure 1B). *HK1.ras* papillomas (Figure 1C) maintained this ordered differentiation profile, with supra-basal 14-3-3 $\sigma$ /K1 expression, but now displayed a significant, almost threefold increase ( $p < 0.001$ ) in basal-layer 14-3-3 $\sigma$  expression (OD:  $61 \pm 9.4$ ), compared to hyperplasia (OD:  $29 \pm 6.4$ ); hence, an orange appearance to 14-3-3 $\sigma$ /K14 IF versus red of K1/K14 basal layers (Figure 1C). Papilloma keratinocytes now expressed uniform, nuclear p53 in both proliferative basal (OD:  $107 \pm 9.4$ ) and supra-basal keratinocytes (OD:  $105 \pm 10.4$ ) which was significantly increased (fourfold;  $p < 0.0001$ ) over earlier hyperplasia (Figure 1B) with low/cytoplasmic p53 (supra-basal OD:  $22 \pm 6.4$ ; basal OD:  $30 \pm 5.4$ ). However, there was little increase in p21 (Figure 1B: basal OD:  $17 \pm 4.4$  vs. Figure 1C: basal OD:  $29 \pm 7.4$ ). This 14-3-3 $\sigma$ -associated p53 expression increase may reflect a lack of spontaneous *HK1.ras* papilloma conversion, consistent with activated p-MDM2<sup>166</sup> being confined to supra-basal layers, alongside low p-AKT1<sup>473</sup> (below; Figures 5 and 6).

### 3.2 | *HK1.fos-Δ5PTEN*<sup>flx/flx</sup> KAs exhibit basal-layer 14-3-3 $\sigma$ associated with elevated p53/p21 and accelerated, anomalous differentiation

Previously, *HK1.fos* cooperation with inactivation of PTEN-mediated AKT regulation (*K14.creP-Δ5PTEN*<sup>flx/flx</sup>) produced keratotic hyperplasia in *HK1.fos-Δ5PTEN*<sup>flx/flx</sup> that evolved into KA (Supporting Information: Figure S2E), as compensatory p53/p21 expression halted proliferation and accelerated differentiation.<sup>28</sup> Analysis of 14-3-3 $\sigma$  in *HK1.fos-Δ5PTEN*<sup>flx/flx</sup> hyperplasia (Figure 2A,B) showed basal-layer keratinocytes exhibited strong, membranous/cytoplasmic expression, accompanied by elevated supra-basal (cytoplasmic) p53 (but not p21, which appeared later) (Figure 2A).<sup>28</sup> Image quantitation of *HK1.fos-Δ5PTEN*<sup>flx/flx</sup> hyperplasia confirmed significant increases in basal-layer 14-3-3 $\sigma$  expression (IHC:  $77 \pm 11$ ; IF:  $73 \pm 12$ ) compared to *HK1.ras* hyperplasia (Figure 1B IF:  $30 \pm 6$ ;  $p < 0.0006$ ). This was reflected by increased supra-basal p53 (Figure 2B IHC supra-basal:  $45 \pm 6.5$ ; basal:  $28 \pm 9.5$ ) versus *HK1.ras* hyperplasia (Figure 1B IHC supra-basal:  $22 \pm 5.4$ ; basal:  $30 \pm 5.4$ ) but not basal-layer p53, consistent with the previously observed requirement for a threshold level of AKT-mediated, p-GSK3 $\beta$  inactivation being necessary to trigger compensatory p53 (and p21) expression.<sup>28</sup>

This suggested basal-layer 14-3-3 $\sigma$  increases were separate to p53, possibly concerned with spatial awareness. Indeed, in the context of *HK1.fos-Δ5PTEN*<sup>flx/flx</sup> hyperplasia, such elevated basal-layer 14-3-3 $\sigma$  was not accompanied by increased keratin K1 (Figure 2B K1 basal layer:  $17 \pm 7.4$ ; see Supporting Information: Figure S7C), which remained similar to *HK1.ras* hyperplasia (Figure 1B K1 basal:  $16 \pm 4.7$ ), suggesting either roles linked to spatial awareness rather than differentiation,<sup>5</sup> or as a direct consequence of activated v-fos expression corrupting endogenous c-fos roles in differentiation.<sup>28</sup>

On progression to KA, two distinct *HK1.fos-Δ5PTEN*<sup>flx/flx</sup> histotypes emerged<sup>28</sup>: a massive keratosis, interspersed with fronds of keratinocytes; and an initial proliferative pathology often confused with wdSCC (Supporting Information: Figure S2E). Analysis of frond-like histotypes (Figure 2C; see Supporting Information: Figure S3), found that elevated 14-3-3 $\sigma$  in both supra-basal (OD:  $89 \pm 13.5$ ) and basal-layer keratinocytes (OD:  $61 \pm 11$ ) was paralleled by strong p53 expression in frond-like basal ( $86 \pm 11$ ) and supra-basal layers ( $55 \pm 9.4$ ). Furthermore, together with elevated p21 in basal-layer ( $78 \pm 13.5$ ) and supra-basal layers ( $47 \pm 9.5$ ), overt KA expressed anomalous keratin K1 in basal-layers (Figure 2C KA frond-like basal:  $103 \pm 19.5$ ; KA frond-like supra-basal:  $104 \pm 18.5$ ), consistent with accelerated, anomalous differentiation and the resultant keratosis observed previously.<sup>28</sup>

In contrast, proliferative basal-layer keratinocytes of wdSCC-like histotypes exhibited low 14-3-3 $\sigma$  expression (Figure 2C: wdSCC-like basal OD:  $29 \pm 8$ ) compared to frond-like areas ( $p < 0.003$ ); yet with similar supra-basal expression (OD:  $79 \pm 21.9$ ). This was paralleled by lower p53 expression (wdSCC-like basal:  $46 \pm 9.9$ ; wdSCC-like supra-basal:  $45 \pm 7.9$ ) and p21 (wdSCC-like basal:  $37 \pm 21.9$ ; wdSCC-like supra-basal:  $40 \pm 9.9$ ); yet here a relatively normal K1 expression profile indicated a benign KA histotype (wdSCC-like basal layer:  $25 \pm 21.9$ ; wdSCC-like supra-basal layer:  $94 \pm 20.9$ ). Hence, increased p53/p21 now combined with 14-3-3 $\sigma$  differentiation functions and cell cycle inhibition<sup>4-6</sup> to evoke a switch from proliferation to (accelerated) differentiation,<sup>28</sup> highlighted by anomalous/premature basal layer keratin K1 expression (Figure 2C: lower end panel) and AKT inhibition (see below) thus avoiding progression to malignancy.<sup>28</sup>

### 3.3 | Early *HK1.ras/fos-Δ5PTEN*<sup>flx/flx</sup> carcinomas show persistent 14-3-3 $\sigma$ following p53 loss which may limit progression in collaboration with p21

In *HK1.ras/fos-Δ5PTEN*<sup>flx/flx</sup> mice, co-operation between *HK1.ras/fos* and loss of PTEN-mediated AKT regulation resulted in rapid papillomatogenesis, however malignant conversion required p53 loss and progression stalled at a wdSCC histotype due to persistent p21 (30; Supporting Information: Figure S2C). Analysis of 14-3-3 $\sigma$  in *HK1.ras/fos-Δ5PTEN*<sup>flx/flx</sup> papillomas (Figure 3A,B IHC; Supporting Information: Figure S7D) showed high levels in proliferative basal-layers (OD Figure 3A:  $67 \pm 9.7$ ; Figure 3B\*:  $74 \pm 9.8$ ; Figure 3B\*\*:  $57 \pm 8.8$ ); again paralleled by elevated p53 (Figure 3A:  $48 \pm 3.7$ ) and p21 (Figure 3A:  $77 \pm 6.7$ ). However, in late-stage *HK1.ras/fos-Δ5PTEN*<sup>flx/flx</sup> papillomas, p53 expression became reduced (Figure 3B\*:  $46 \pm 8.9$  [ $p < 0.0007$ ]) and expression was lost in specific areas (Figure 3B\*\*:  $25 \pm 8.7$ ); hence loss of p53 guardianship increased spontaneous mutations leading to wdSCC (Figure 3B high magnification:  $11 \pm 9$  [significance vs. Figure 3B\*:  $p < 0.0003$ ; vs. Figure 3B\*\*:  $p < 0.001$ ], see Supporting Information: Figure S4A).

In contrast, in both late-stage papilloma and wdSCC histotypes, 14-3-3 $\sigma$  and p21 remained elevated (Figure 3B\* 14-3-3 $\sigma$ :  $74 \pm 9.4$ ; Figure 3B\* p21:  $89 \pm 8.1$ ); and moreover, 14-3-3 $\sigma$  expression remained in areas of reduced p53 (Figure 3B\*\*:  $55 \pm 6.7$

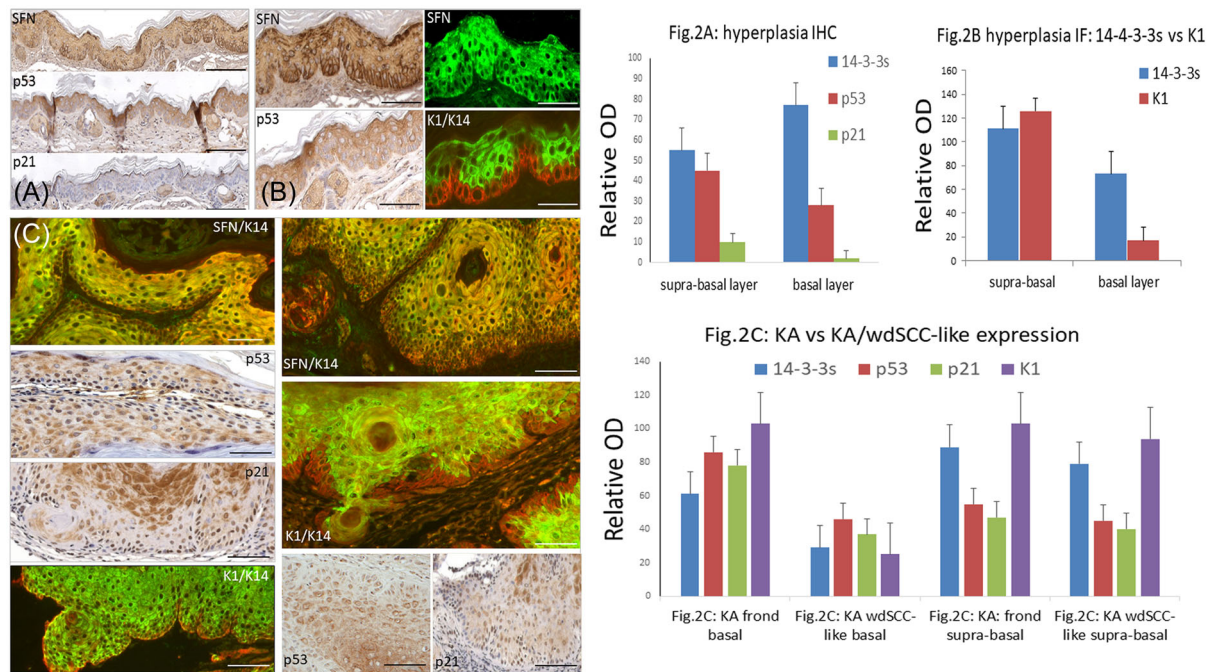


**FIGURE 2** 14-3-3 $\sigma$ , p53 and p21 expression in *HK1.fos- $\Delta$ 5PTEN<sup>flx/flx</sup>* keratoacanthoma etiology. (A) *HK1.fos/ $\Delta$ 5PTEN<sup>flx/flx</sup>* hyperplasia shows elevated basal layer 14-3-3 $\sigma$  expression with mainly cytoplasmic p53 expression in supra-basal keratinocytes, whereas p21 is expressed at low levels. (B) At higher magnification, both IHC and IF analysis show elevated basal-layer 14-3-3 $\sigma$  expression is cytoplasmic and membranous; similarly elevated p53 appears mainly cytoplasmic with sporadic nuclear expression and K1 expression remains normal. (C) Left panels: *HK1.fos/ $\Delta$ 5PTEN<sup>flx/flx</sup>* keratoacanthoma shows the highly differentiated, frond-like histopathology (see Supporting Information: Figure S2E) exhibits strong basal- and supra-basal 14-3-3 $\sigma$  expression, paralleled by elevated, nuclear p53 and p21; where anomalous basal-layer K1 expression indicates premature differentiation.<sup>28</sup> In contrast, less-differentiated, wdSCC-like keratoacanthoma histopathology (right panels) exhibits weaker and mainly supra-basal 14-3-3 $\sigma$ /K1 expression, paralleled by lower p53/p21. Right: Image J quantitation of hyperplasia confirms elevated basal- and supra-basal 14-3-3 $\sigma$  expression, with elevated p53 but little p21. Analysis of KA histotypes shows high expression of each protein in areas of highly differentiated histotypes – including anomalous K1 expression in basal layers; whereas wdSCC-like histotypes exhibit lower basal-layer expression, yet 14-3-3 $\sigma$  and K1 expression persists in the supra-basal layers as observed in wdSCC. Bars: (A) approximately 120–150  $\mu$ m; (B) IHC: 14-3-3 $\sigma$ /p53 approximately 75  $\mu$ m; IF: 14-3-3 $\sigma$  approximately 50  $\mu$ m; K1/K14 approximately 30  $\mu$ m; (C) Left column: 14-3-3 $\sigma$ /p53/p21 approximately 60–75  $\mu$ m; K1/K14 approximately 100  $\mu$ m. Right column: 14-3-3 $\sigma$ /p53 approximately 60–75  $\mu$ m; K1/K14 approximately 50  $\mu$ m; p21 approximately 100  $\mu$ m. wdSCC, well-differentiated squamous cell carcinoma.

[ $p < 0.0005$ ]) and persisted in p53-negative wdSCC (Figure 3B:  $52 \pm 5.7$  [ $p < 0.0001$ ]); albeit at reduced levels, possibly reflecting 14-3-3 $\sigma$  expression regulation by p53.<sup>4</sup> Similarly, p21 persisted (Figure 3B<sup>\*\*</sup>:  $67 \pm 6.7$  [vs. p53:  $p < 0.0005$ ]) and expression actually increased following conversion to p53-negative wdSCC (Figure 3B:  $87 \pm 8.7$  [vs. p53 wdSCC:  $p < 0.0001$ ]; see Supporting Information: Figure S4A); again suggesting a feedback to p53 loss that, alongside persistent 14-3-3 $\sigma$ , helped inhibit progression<sup>29</sup> until lost during development of aggressive SCC (see Figure 6 and Supporting Information: Figure S4A, lane 14).

Immunofluorescence analysis of *HK1.ras/fos- $\Delta$ 5PTEN<sup>flx/flx</sup>* tumors possessing papilloma, wdSCC and SCC histotypes (Figure 3C, see Supporting Information: Figure S7E) also showed that strong 14-3-3 $\sigma$  expression in papillomas (Figure 3A OD:  $125 \pm 15.1$ ) became reduced in late-stage papilloma (Figure 3C [low mag. green] OD:  $107 \pm 13.3$  [vs. 3A:  $p < 0.02$ ]), yet expression persisted following conversion to (p53-negative) wdSCC (Figure 3C wdSCC [low mag. yellow area] OD:  $64 \pm 10.1$  [ $p < 0.005$ ]); until lost on progression to SCC (Figure 3C [low mag.] OD:  $34 \pm 7.6$  [ $p < 0.0005$ ]). At higher magnification,

compared to papilloma basal-layer 14-3-3 $\sigma$  expression (Figure 3A IF:  $91 \pm 20.5$ ), wdSCCs showed invasive basal-layer keratinocytes exhibited significantly reduced 14-3-3 $\sigma$  levels (Figure 3C [arrows] wdSCC1:  $37 \pm 8.6$ ; wdSCC2:  $35.5 \pm 6.6$  [ $p < 0.0001$ ]) consistent with loss of a TSG role during invasion and progression (see K1 analysis for histotype conformation; Supporting Information: Figure S5). Hence, larger areas of reduced 14-3-3 $\sigma$  expression and eventual loss (Figure 3C SCC1:  $29 \pm 12.2$ ; SCC2:  $26 \pm 11.9$ ) drove SCC progression. Of note, 14-3-3 $\sigma$  loss was paralleled by p21 loss and increased p-AKT1<sup>473</sup>; suggesting this was a key interaction during malignant progression – a result also repeated in TPA promotion experiments.

### 3.4 | Rapid tumor progression in TPA-treated *HK1.ras- $\Delta$ 5PTEN<sup>flx/flx</sup>* carcinogenesis associates with early loss of 14-3-3 $\sigma$ , p53 and p21

Previously, a lack of tumor progression in *HK1.ras- $\Delta$ 5PTEN<sup>flx/flx</sup>* studies<sup>27</sup> had prompted TPA promotion experiments, which resulted

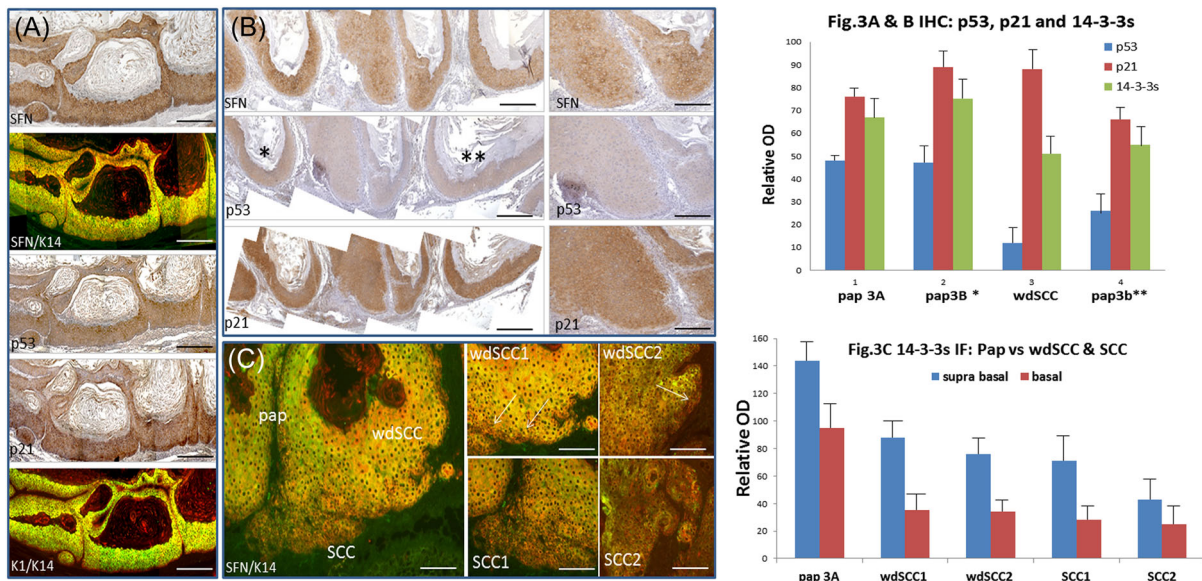


**FIGURE 3** 14-3-3 $\sigma$ , p53 and p21 expression in *HK1.ras/fos-Δ5PTEN<sup>flx/flx</sup>* SCC etiology. *Left panel:* (A) Early *HK1.ras/fos-Δ5PTEN<sup>flx/flx</sup>* papillomas exhibit strong basal and granular layer 14-3-3 $\sigma$  expression; with a hiatus in the intermediate, acanthotic layers. Strong p53 is observed in all layers; while basal p21 expression parallels 14-3-3 $\sigma$ , with lower levels in acanthotic layers. Supra-basal K1 expression indicates benign tumor. (B) IHC analysis of typical mixed histotype *HK1.ras/fos-Δ5PTEN<sup>flx/flx</sup>* tumor shows elevated 14-3-3 $\sigma$ /p21 co-expression; whereas p53 is reduced in papilloma histotypes (\*) and absent in areas of converting papilloma (\*\*). Higher magnification (used for quantitation) of wdSCC histotype shows persistent (if lower) 14-3-3 $\sigma$  expression alongside maintained p21 expression and p53 loss. (C) IF analysis of mixed *HK1.ras/fos-Δ5PTEN<sup>flx/flx</sup>* tumor shows elevated 14-3-3 $\sigma$  expression in papilloma histotypes (green) persists in wdSCC histotypes (yellow) but weakens in invasive SCC areas (red due to K14 counterstain). At higher magnification wdSCC histotypes exhibit reduced 14-3-3 $\sigma$  in the invasive basal layers (arrows wdSCC 1 and 2) with further, more uniform regression in SCC1 which is finally lost on progression to more aggressive SCC (SCC2) (Quantitation shown in Figure 4 below). *Right panel:* Image J quantitation of IHC analysis shown in (B), confirms persistence of 14-3-3 $\sigma$  and p21 following conversion to wdSCC whereas p53 expression diminished in papillomas (\*\*) and was lost in wdSCC. Lower: Image J quantitation of IF analysis shown in (C) demonstrates reduction and loss of 14-3-3 $\sigma$  expression in basal versus suprabasal keratinocytes of papillomas, wdSCC and SCC. Bars (A) approximately 120–150  $\mu$ m; (B) Left: approximately 120–150  $\mu$ m. Right: approximately 100  $\mu$ m; (C) approximately 100 and 75  $\mu$ m. SCC, squamous cell carcinoma; wdSCC, well-differentiated SCC.

in rapid progression to aggressive SCC/pdSCC<sup>27</sup> (see Supporting Information: Figure S2D). Immunofluorescence analysis (Figure 4), demonstrated that SCC/pdSCC tumors lacked detectable 14-3-3 $\sigma$  expression (Figure 4A:  $17 \pm 8.5$ ), while the areas of TPA-promoted *HK1.ras-Δ5PTEN<sup>flx/flx</sup>* hyperplasia already exhibited reduced expression (Figure 4A supra-basal:  $63 \pm 10.5$ ; basal:  $38 \pm 11.6$ ; see Supporting Information: Figure S5), compared to typical papillomas (Figure 3A IF supra-basal:  $142 \pm 23.5$  [ $p < 0.001$ ]; basal:  $91 \pm 20.5$  [ $p < 0.0007$ ]). Indeed, hyperplastic basal-layer 14-3-3 $\sigma$  expression was already reduced to levels observed in wdSCCs (e.g., wdSCC1:  $37 \pm 8.6$ ).

Thus, any initial 14-3-3 $\sigma$ -mediated suppressive responses to inhibit papillomatogenesis (alongside p53 and p21) were short lived, as more sensitive IHC analysis of TPA-promoted *HK1.ras-Δ5PTEN<sup>flx/flx</sup>* tumors (Figure 4B) showed 14-3-3 $\sigma$  loss in K1-positive papilloma ( $17 \pm 2.6$ ), resulting in 14-3-3 $\sigma$ -negative pdSCC ( $11 \pm 3.6$ ), was paralleled by complete p53 ( $4.3 \pm 6.6$ ) and p21 ( $7 \pm 3.6$ ) loss (Figure 4B). Similarly, IHC analysis of TPA-promoted *HK1.ras-Δ5PTEN<sup>flx/flx</sup>* hyperplasia showed early loss of TSG expression (Figure 4C: 14-3-3 $\sigma$  upper:  $19 \pm 6.6$ ; lower:  $31 \pm 6.4$ ; p53 upper:  $14 \pm 4.6$ ; lower:  $21 \pm 3.4$ ; p21 upper:  $16 \pm 6.6$ ; lower:  $28 \pm 6.4$ ),

consistent with rapid progression to pdSCC (see Supporting Information: Figure S5 for quantitation and K1 expression analysis).

### 3.5 | *HK1.ras/fos-Δ5PTEN<sup>flx/flx</sup>* tumor progression highlights 14-3-3 $\sigma$ /p-MDM2<sup>166</sup> antagonism in p53-associated malignant conversion

Given the antagonistic 14-3-3 $\sigma$  and MDM2 interactions involved in p53 regulation,<sup>3,4,22</sup> activated p-MDM2<sup>166</sup> status was investigated in stage-specific tumor etiology (Figure 5). In normal epidermis, activated p-MDM2<sup>166</sup> expression paralleled p53 and 14-3-3 $\sigma$  in being supra-basal, with occasional positive basal expression in cycling keratinocytes alongside sporadic p53/14-3-3 $\sigma$  (Figure 5A: p-MDM2<sup>166</sup> supra-basal:  $48 \pm 3.5$ ; basal:  $26 \pm 3.5$ ; 14-3-3 $\sigma$  [IF] supra-basal:  $42 \pm 6.5$ ; basal:  $24 \pm 3.5$ ; p53 supra-basal:  $28 \pm 6.5$ ; basal:  $28 \pm 8.5$ ). Similarly, *HK1.ras* papillomas displayed elevated, supra-basal p-MDM2<sup>166</sup> (Figure 5B: supra-basal:  $107 \pm 29.5$ ), alongside elevated 14-3-3 $\sigma$  expression ( $108 \pm 16.5$ ); possibly geared to maintain lower p53 levels ( $30 \pm 7.5$ ) and avoid anomalous p53-mediated apoptosis that might compromise barrier functions.<sup>27,28</sup>

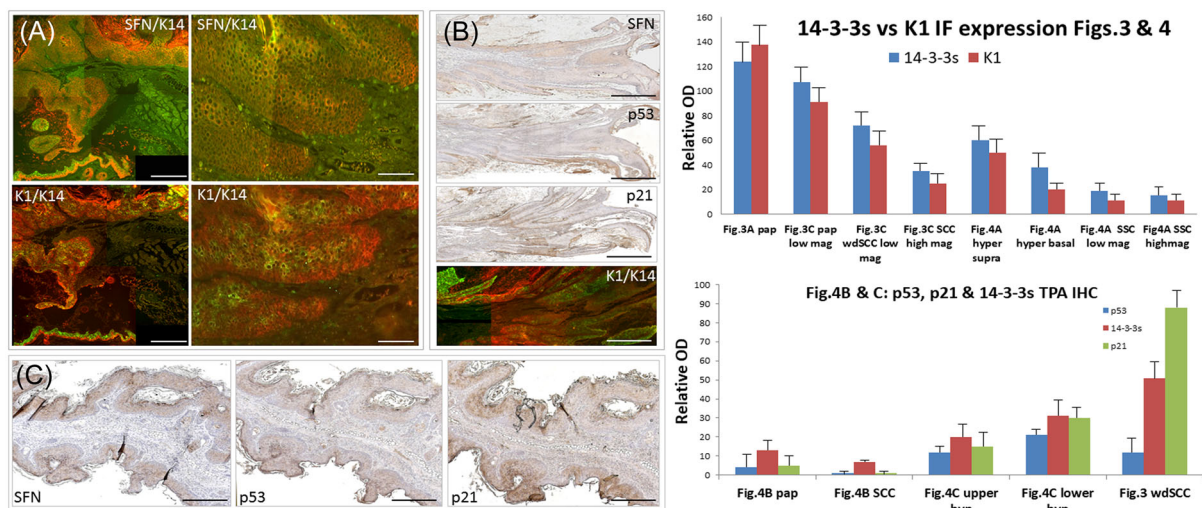


**FIGURE 4** 14-3-3 $\sigma$ , p53 and p21 expression in TPA-promoted, poorly differentiated SCC. (A) Low and high magnification immunofluorescence analysis of a typical TPA-promoted *HK1.ras-Δ5PTEN<sup>flx/flx</sup>* pdSCC shows loss of 14-3-3 $\sigma$  expression, alongside K1 loss, compared to adjacent epidermal hyperplasia (bottom left). (B) IHC analysis of earlier TPA-promoted *HK1.ras-Δ5PTEN<sup>flx/flx</sup>* papilloma/wdSCC/SCC also shows 14-3-3 $\sigma$  loss parallels loss of p53 and p21; even in areas of K1-positive papilloma. (C) IHC analysis of TPA-promoted *HK1.ras-Δ5PTEN<sup>flx/flx</sup>* hyperplasia already shows loss of 14-3-3 $\sigma$  parallels p53 loss and reduced p21 (see Supporting Information: Figure S2D). Right panels: Upper: Image J quantitation of IF analysis tumor histotypes in Figures 3 and 4A confirms reduced expression of 14-3-3 $\sigma$  and keratin K1 as papillomas (Figure 3A) convert to wdSCC (Figure 3C) and such reduced levels were already demonstrated in TPA-promoted hyperplasia (Figure 4A; Supporting Information: Figure S5). Lower panel: Quantitation of Figure 4B,C IHC analysis shows TPA treated papillomas and SCCs lacked 14-3-3 $\sigma$ , p53 and p21; while TPA-promoted *HK1.ras-Δ5PTEN<sup>flx/flx</sup>* hyperplasia again expressed loss compared to persistent 14-3-3 $\sigma$  and p21 observed in wdSCC (Figure 3B; see also Supporting Information: Figure S5). Bars (A) approximately 120–150 and 50  $\mu$ m; (B) approximately 150  $\mu$ m; (C) approximately 100  $\mu$ m. pdSCC, poorly differentiated SCC; SCC, squamous cell carcinoma; wdSCC, well-differentiated SCC.

In larger *HK1.ras* papillomas where p-MDM2<sup>166</sup> was detectable in strands of basal-layer keratinocytes, expression was mainly cytoplasmic not nuclear (Figure 5B: 42 ± 13.5), reflecting increased 14-3-3 $\sigma$  (Figure 5B: 60 ± 3.5), which acted to chaperone MDM2 into the cytoplasm for ubiquitination.<sup>3,4,22</sup> Hence, *HK1.ras* papillomas lacked activated, nuclear p-MDM2<sup>166</sup> which resulted in elevated nuclear p53 (Figure 5B: 68 ± 10.5) and this significant increase over normal ( $p < 0.0001$ ) helped prevent malignant conversion.<sup>27,33</sup> In triple *HK1.ras/fos-Δ5PTEN<sup>flx/flx</sup>* papillomas (Figure 5C), elevated basal-layer 14-3-3 $\sigma$  (51 ± 20.4) again appears geared to sequester activated p-MDM2<sup>166</sup> to supra-basal keratinocytes (77 ± 7.4); and any potential increase in basal-layer p-MDM2<sup>166</sup> expression (48 ± 8.4) remained destined for cytoplasmic ubiquitination. Thus, basal-layer keratinocytes were mainly negative for nuclear p-MDM2<sup>166</sup> (Figure 5C; papilloma panels) and consequently at this stage, nuclear p53 levels remained high (77 ± 5.4).

However, with time, in *HK1.ras/fos-Δ5PTEN<sup>flx/flx</sup>* tumors comprised of papilloma, wdSCC and SCC histotypes (above, Figure 3C), strong nuclear p-MDM2<sup>166</sup> expression appeared in all layers of wdSCC and SCC histotypes (Figure 5C: left and middle panels: wdSCC: 77 ± 11.4; SCC: 91 ± 9.4 [vs. papilloma  $p < 0.0002$ ]). This supra-basal-to-basal expression of activated p-MDM2<sup>166</sup> in wdSCC was paralleled by a reverse, basal-to-supra-basal reduction in 14-3-3 $\sigma$  (Figure 5C wdSCC basal: 35 ± 5.4 [vs. papilloma  $p < 0.0005$ ]) and loss of p53 (21 ± 4.4

[ $p < 0.0003$ ]); while continued expression of p-MDM2<sup>166</sup> in SCCs corresponded loss of 14-3-3 $\sigma$  expression (basal: 24 ± 6.9 [ $p < 0.0001$ ]) and virtually undetectable p53 (basal: 14 ± 4.1 [ $p < 0.0001$ ]). Similar 14-3-3 $\sigma$  loss was observed in vitro, where 3D raft cultures of invasive SCC and melanoma cells were negative for 14-3-3 $\sigma$  expression, unlike their cultured 2D counterparts (see Figure 7). Thus, in *HK1.ras/fos-Δ5PTEN<sup>flx/flx</sup>* carcinogenesis, reduced basal-layer 14-3-3 $\sigma$  and subsequent increased p-MDM2<sup>166</sup> activity, lowered p53 levels giving a susceptibility to malignant conversion/progression.

### 3.6 | 14-3-3 $\sigma$ /p21 co-operation inhibits AKT to limit malignant progression

Analysis of *HK1.ras/fos-Δ5PTEN<sup>flx/flx</sup>* SCC and TPA-promoted *HK1.ras-Δ5PTEN<sup>flx</sup>* pdSCCs etiology showed a distinct 14-3-3 $\sigma$ /p21 co-expression profile that appeared to antagonize p-AKT1<sup>473</sup> and limit malignant progression (Figure 6). Initially, in *HK1.ras/fos-Δ5PTEN<sup>flx/flx</sup>* papillomas (Figure 6A), elevated 14-3-3 $\sigma$ /p21 co-expression in basal and supra basal layers (14-3-3 $\sigma$  basal: 88 ± 4.4; 14-3-3 $\sigma$  supra-basal: 75 ± 3.6; p21 basal: 97 ± 7.4; p21 supra-basal: 72 ± 9.4) was associated with low p-AKT1<sup>473</sup> expression (basal: 22 ± 12.4; supra-basal: 18 ± 5.4). This suggested initial responses to loss of PTEN-mediated AKT regulation, including

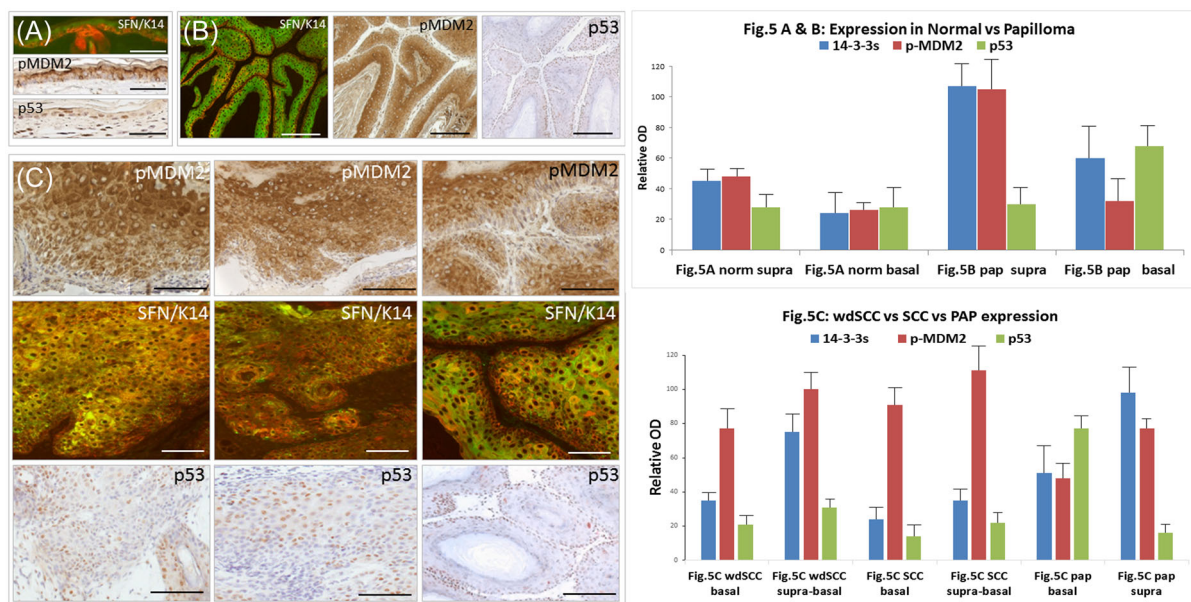


**FIGURE 5** p-MDM2<sup>166</sup> and 14-3-3σ/p53 expression in *HK1.ras* papilloma and *HK1.ras/fos-Δ5PTEN<sup>flx/flx</sup>* SCC etiology. (A) Normal epidermis shows supra-basal 14-3-3σ parallels activated p-MDM2<sup>166</sup> expression, with sporadic positive basal-layer keratinocytes also observed for p53. (B) *HK1.ras* papilloma sections show supra-basal 14-3-3σ parallels supra-basal p-MDM2<sup>166</sup> expression, but with increasing nuclear p53 appearing in basal layer keratinocytes. (C) Left column: *HK1.ras/fos-Δ5PTEN<sup>flx/flx</sup>* wdSCCs show elevated basal layer p-MDM2<sup>166</sup> expression, while 14-3-3σ remains essentially supra-basal and p53 becomes sporadic. Middle column: Aggressive *HK1.ras/fos-Δ5PTEN<sup>flx/flx</sup>* SCC/pdSCC shows strong p-MDM2<sup>166</sup> expression in invasive SCC keratinocytes; while 14-3-3σ becomes sporadic alongside occasional p53-positive cells. Right column: For comparison *HK1.ras* papilloma exhibits supra-basal 14-3-3σ/p-MDM2<sup>166</sup> and nuclear p53-positive basal-layer keratinocytes. Bars (A) approximately 25–30 μm; (B) approximately 85–100 μm; (C) wdSCC and pdSCC approximately 50–75 μm. pdSCC, poorly differentiated SCC; SCC, squamous cell carcinoma; wdSCC, well-differentiated SCC.

high p53 levels (above; Figure 3A), inhibited p-AKT1<sup>473</sup> expression. Further, despite p53 loss in *HK1.ras/fos-Δ5PTEN<sup>flx/flx</sup>* wdSCCs (Figure 6B), persistent basal/suprabasal-layer 14-3-3σ/p21 co-expression (14-3-3σ basal: 51 ± 2.4; supra-basal: 86 ± 3.2; p21 basal: 70 ± 13.9; supra-basal: 64 ± 5.5) appeared to confine any increase in p-AKT1<sup>473</sup> expression to supra-basal wdSCC layers (basal: 17 ± 4.3; supra-basal: 53 ± 5.4).

As wdSCC *HK1.ras/fos-Δ5PTEN<sup>flx/flx</sup>* tumors progressed to aggressive SCC (Figure 6C), reduced 14-3-3σ was paralleled by reduced p21 expression, particularly in the invasive basal layers (14-3-3σ basal: 13 ± 12.4; supra-basal: 38 ± 8.2; p21 basal: 17 ± 5.3; supra-basal: 48 ± 2.5), which corresponded to increased, activated p-AKT1<sup>473</sup> becoming widely expressed in all layers (basal: 48 ± 12.5; supra-basal: 70 ± 11.9). This antagonism was also demonstrated in TPA-promoted, *HK1.ras-Δ5PTEN<sup>flx/flx</sup>* pdSCC etiology (Figure 6D). Here, early loss of 14-3-3σ/p21 expression (14-3-3σ basal: 10 ± 2.4; supra-basal: 38 ± 5.4; p21 basal: 20 ± 4.3; supra-basal: 7 ± 4.1) coupled to p53 loss (Figure 4C p53: basal 14 ± 4.6), gave high levels of p-AKT1<sup>473</sup> expression (basal: 71 ± 5.5; supra-basal: 89 ± 12.9) consistent with rapid papillomatogenesis, conversion and progression to pdSCC. Taken collectively, these data indicate a strong synergism exists between 14-3-3σ and p21, possibly geared to inhibit AKT-mediated progression following p53 loss; and this aspect is under further investigation in p21 knockout and inducible 14-3-3σ knockout models.

### 3.7 | 14-3-3σ persists in malignant SCC cells grown in 2D but not invasive cells of 3D-cultures

To compare in vivo findings to cultured cells (Figure 7), 14-3-3σ expression was assessed in immortalized HaCaT keratinocytes<sup>34</sup>; ras<sup>Ha</sup>-transformed (DMBA/TPA) SP1 papilloma cells (SP1<sup>ras61</sup>); and T52 SCC cells, derived from SP1 keratinocytes transformed by v-fos (T52<sup>ras61/HVVfos</sup>).<sup>37</sup> Initially, 14-3-3σ was assessed in transformation assays via resistance to calcium induced differentiation. Here, SP1<sup>ras61</sup> cells adopted a flattened morphology consistent with attempts to differentiate; while T52<sup>ras61/HVVfos</sup> cells were indifferent to raised calcium levels, consistent with their SCC phenotype (Supporting Information: Figure S6).

In 2D cultures, membranous/cytoplasmic 14-3-3σ expression was detected in immortalized HaCaT and SP1<sup>ras61</sup> papilloma keratinocytes cultured in proliferative Low Calcium (0.05 mM Ca<sup>2+</sup>) media, giving a halo appearance (upper panel; Figure 7), consistent with roles in spatial awareness/contact inhibition<sup>19,20,22</sup> and immortalized/benign tumor phenotypes observed in vivo. However, 14-3-3σ expression was also observed in malignant T52<sup>ras61/v-fos</sup> SCC keratinocytes, with a similar cytoplasmic halo appearance, which may reflect expression observed in malignant *HK1.ras/fos-Δ5PTEN<sup>flx/flx</sup>* wdSCCs (above). When challenged to differentiate in high calcium media (>0.12 mM Ca<sup>2+</sup>), increased numbers of SP1<sup>ras61</sup> keratinocytes exhibited 14-3-3σ with expression in distinct cytoplasmic areas; consistent with roles in spatial awareness. T52<sup>ras61/v-fos</sup> also

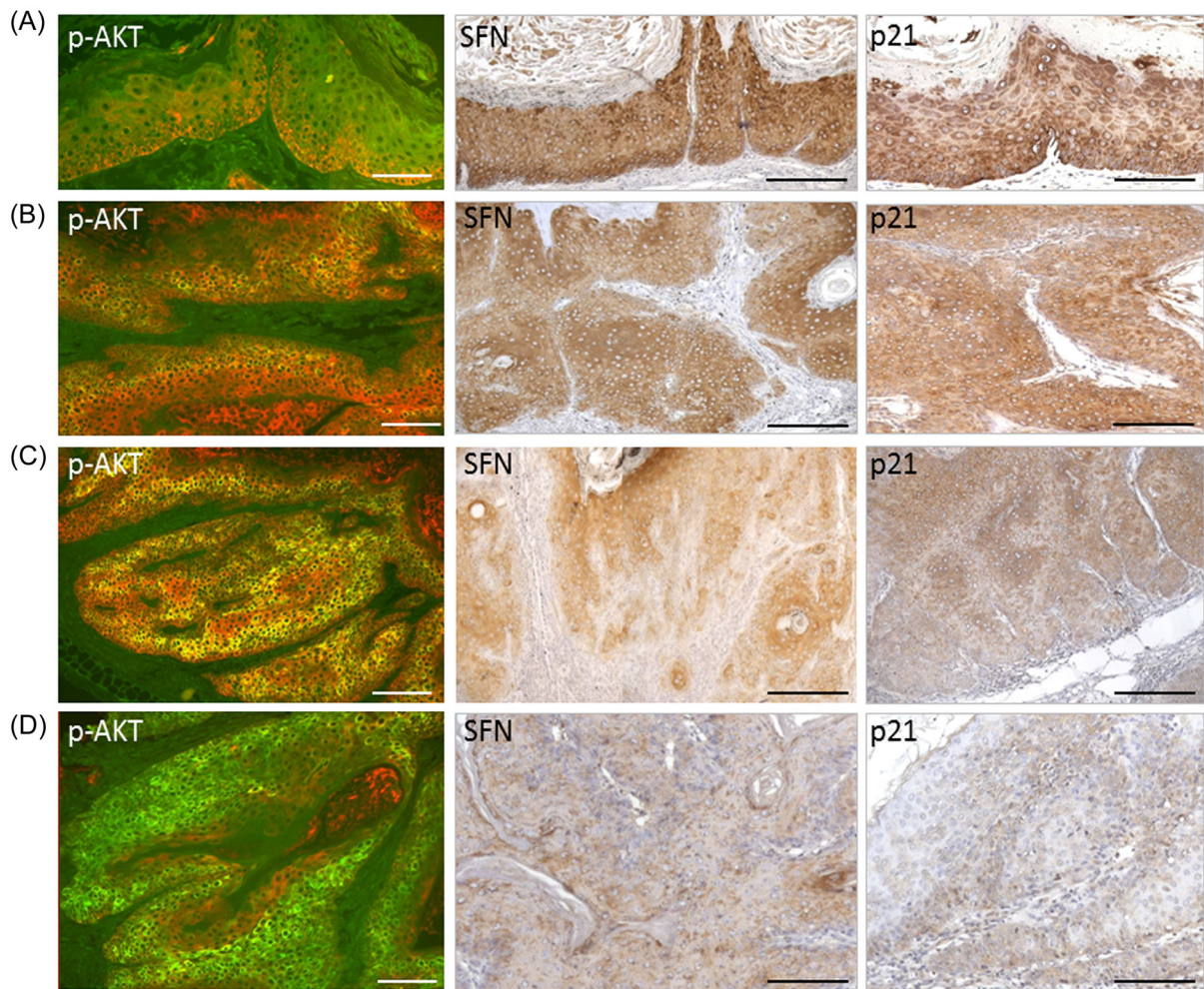


**Fig.6: 14-3-3s, p-AKT1 and p21 in progression**

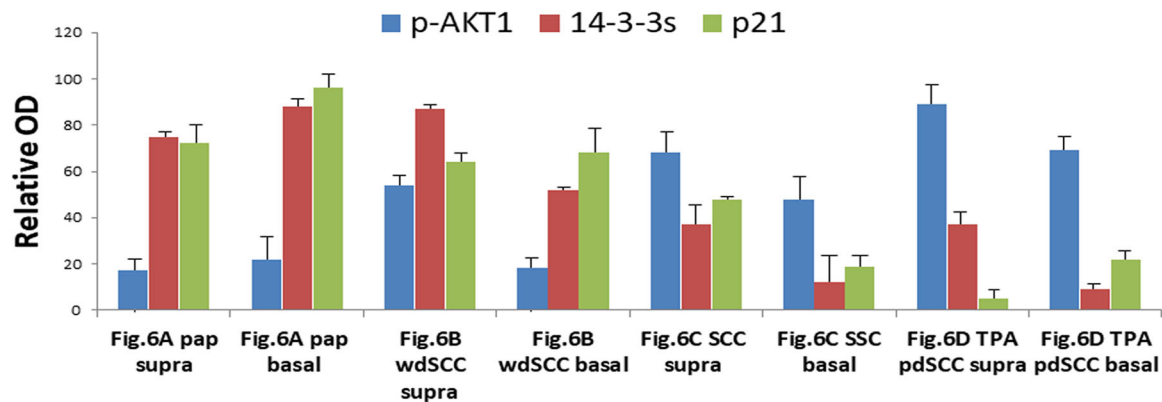


**FIGURE 6** p-AKT1<sup>473</sup> and 14-3-3σ/p21 expression in *HK1.ras/fos-Δ5PTEN<sup>flx/flx</sup>* wdSCC/SCC and TPA-promoted pdSCC etiology. (A) *HK1.ras/fos-Δ5PTEN<sup>flx/flx</sup>* hyperplasia lacks p-AKT1<sup>473</sup> expression alongside basal layer 14-3-3σ and p21 co-expression which become reduced in the upper acanthotic layers. (B) Early, well-differentiated *HK1.ras/fos-Δ5PTEN<sup>flx/flx</sup>* SCCs exhibit increasing p-AKT1<sup>473</sup> but expression is confined to supra-basal layers given continued basal-layer 14-3-3σ/p21 co-expression. (C) Aggressive *HK1.ras/fos-Δ5PTEN<sup>flx/flx</sup>* SCCs exhibit uniform p-AKT1<sup>473</sup> expression in basal layers, paralleled by reduction/loss of 14-3-3σ/p21 expression in invasive keratinocytes. (D) TPA-promoted *HK1.ras-Δ5PTEN<sup>flx/flx</sup>* pdSCC etiology exhibits high uniform p-AKT1<sup>473</sup> expression (i.e., levels mask K14 counterstain); paralleled by loss of 14-3-3σ and p21 expression. Bars approximately 85–100 μm. pdSCC, poorly differentiated SCC; SCC, squamous cell carcinoma; wdSCC, well-differentiated SCC.

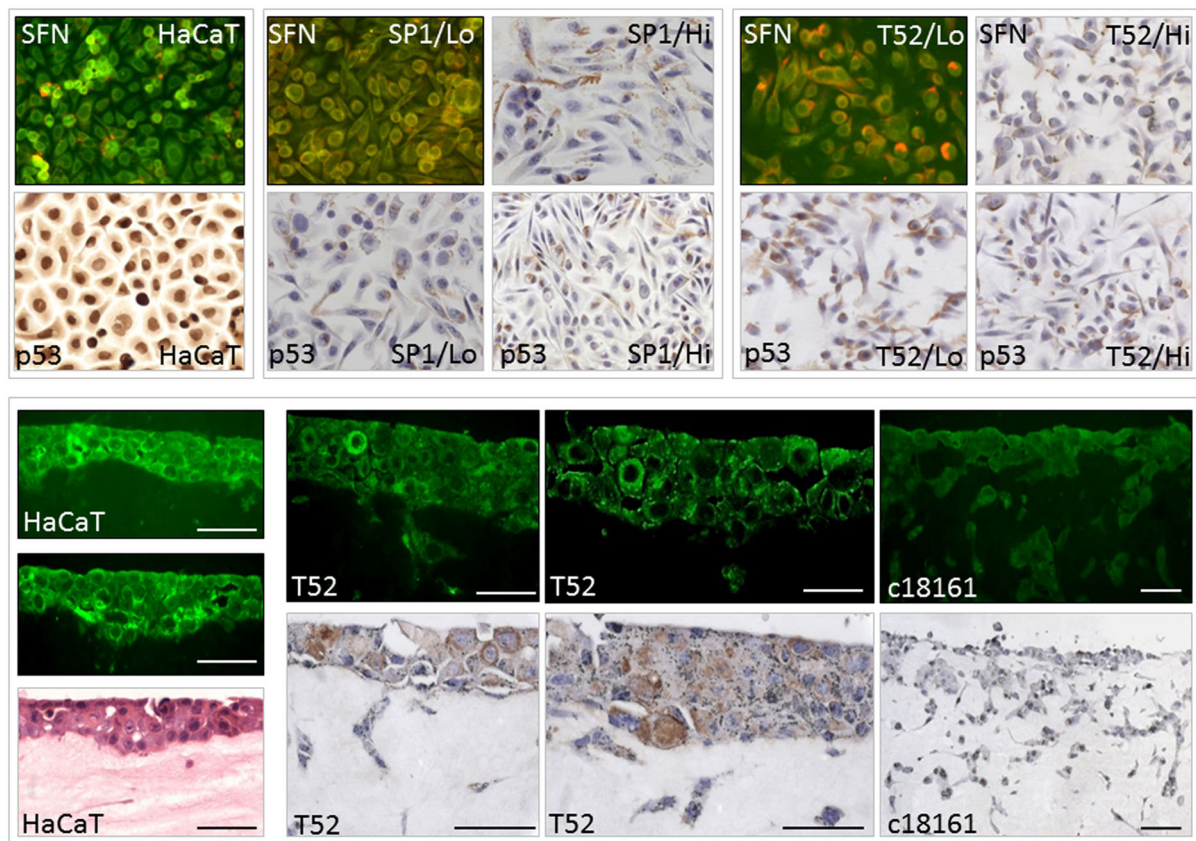


**FIGURE 7** In vitro analysis of 14-3-3 $\sigma$  expression in normal, papilloma, and malignant cells. Upper panel: 2D culture shows immortalized HaCaT keratinocytes express membranous 14-3-3 $\sigma$  and high levels of nuclear p53. Benign SP1<sup>ras61</sup> papilloma cells express membranous 14-3-3 $\sigma$  in proliferative, low Ca<sup>2+</sup> media with spatially localized cytoplasmic expression when differentiating in high Ca<sup>2+</sup> media; accompanied by sporadic, mainly cytoplasmic p53. Malignant T52<sup>ras61/HV<sup>v</sup>fos</sup> cells express less membranous 14-3-3 $\sigma$ /SFN in proliferative low Ca<sup>2+</sup> media; but retained this distinct cytoplasmic localization in high Ca<sup>2+</sup> media, despite being resistant to Ca<sup>2+</sup>-induced differentiation. In both proliferative and differentiating media, T52<sup>ras61/HV<sup>v</sup>fos</sup> cells exhibit cytoplasmic/nuclear levels of p53 (Supporting Information: Figure S3 gives cell morphology). Lower panel: 14-3-3 $\sigma$  expression in 3D tumor invasion assays. HaCaT cells produce a relatively normal skin on organotypic rafts, with membranous 14-3-3 $\sigma$  expression in basal and supra-basal keratinocytes. T52<sup>ras61/v-<sup>fos</sup></sup> SCC cells exhibit weaker expression in sporadic basal layer cells; however, both IF and IHC analysis show invasive T52<sup>ras61/v-<sup>fos</sup></sup> cells lack 14-3-3 $\sigma$  expression. Similarly, the positive invasive control, c18161 melanoma cells are negative for 14-3-3 $\sigma$  expression. Bars: approximately 30–40  $\mu$ m. SCC, squamous cell carcinoma.

exhibited this profile, thus maintaining a spatial awareness, yet suggesting 14-3-3 $\sigma$  had become uncoupled from suppressive functions or had adopted an oncogenic role.

For comparison, p53 expression was strong and nuclear in HaCaT cells,<sup>33</sup> whereas in proliferative Low Cal conditions, sporadic SP1<sup>ras61</sup> cells expressed mainly cytoplasmic p53 which increased in differentiating Hi Cal media. Oddly, malignant T52<sup>ras61/v-<sup>fos</sup></sup> cells expressed p53, but expression was assumed to be a mutant version, based on initiation with DMBA<sup>33</sup> such as the p53<sup>175</sup> GOF mutant.<sup>21</sup> Given that p53 directly induces 14-3-3 $\sigma$  expression,<sup>3,4,22</sup> this observation may also account for 14-3-3 $\sigma$  detection in SCC cells.

In organotypic 3D rafts, the normal skin produced by HaCaT cells displayed 14-3-3 $\sigma$  in basal and supra-basal keratinocytes; with a distinct membranous location indicative of spatial awareness (Figure 7 left panel: single IF staining). Unfortunately, SP1<sup>ras61</sup> cells attempted to create (fragile) papilloma at the air/liquid interface, which were lost in sample

processing. Indeed, collagen-based rafting protocols<sup>36</sup> appeared less optimum for murine SP1/T52 cells compared to human HaCaT or c18161 melanoma cells. However, invasive T52<sup>ras61/v-<sup>fos</sup></sup> SCC cells essentially nailed this model epidermis to the collagen raft (Figure 7: lower panel) where T52 cells exhibited 14-3-3 $\sigma$  expression but this was lost in the invasive cells; as observed for invasive c18161 melanoma cells (Figure 7: lower panel; right). Thus, in vitro data suggest that while TSG functions may be lost during progression/invasion; in certain malignant contexts, persistent 14-3-3 $\sigma$  expression may act to influence tumor outcome.

## 4 | DISCUSSION

In *HK1.ras/fos-Δ5PTEN<sup>flx/flx</sup>* mice overall the in vivo observations were consistent with tumor suppressive roles for 14-3-3 $\sigma$ , where elevated expression interacted with p53/MDM2 during papillomatogenesis to

inhibit malignant conversion; while lower, persistent expression cooperated with p21 to initially inhibit AKT-associated malignant progression. Additionally, as 14-3-3 $\sigma$  acts with CDK-inhibitors p21, p15 and p27 to limit G1/S progression,<sup>38</sup> normal epidermis displayed sporadic 14-3-3 $\sigma$  in dividing (p53/p21 positive) basal-layer keratinocytes; hence, development of epidermal hypoplasia when overexpressed in transgenic mice.<sup>39</sup> Consistent with roles in differentiation, normal epidermis and *HK1.ras* hyperplasia/papillomas expressed supra-basal 14-3-3 $\sigma$ ; further, expression appeared in sporadic populations of narrow, basal-layer keratinocytes that co-expressed keratin K1 (Figure 1A,B); an early marker of epidermal differentiation lost during malignant conversion.<sup>27-29</sup> This suggests roles in keratinocyte commitment to differentiate,<sup>17-19</sup> which require abilities to alter cell shape and migrate,<sup>5</sup> consistent with findings that 14-3-3 $\sigma$  stabilized complexes of keratin intermediate filaments with the actomyosin cytoskeleton<sup>36</sup> to alter cell shape, rigidity and motility; a role potentially subverted in localized tumor invasion.<sup>40</sup> In *HK1.fos- $\Delta$ 5PTEN<sup>flx/flx</sup>* KA etiology, 14-3-3 $\sigma$  expression reinforced roles in differentiation with elevated, membranous expression in hyperplastic *HK1.fos- $\Delta$ 5PTEN<sup>flx/flx</sup>* basal-layer keratinocytes (Figure 2A,B), which resulted in accelerated/premature keratinocyte differentiation,<sup>28</sup> culminating in classic KA keratosis (Supporting Information: Figure S2E). This suggests 14-3-3 $\sigma$  co-operation with *fos* and *PTEN* in regulation of the proliferation/differentiation balance. Indeed given the well-characterized interactions between 14-3-3 $\sigma$ /p53/p21,<sup>3,4,22</sup> as elevated basal-layer 14-3-3 $\sigma$  expression preceded that of p53/p21 (Figure 2A,B), it may help trigger compensatory p53/p21 responses that switched hyperproliferation into the differentiation that dominates KA etiology.<sup>28</sup> Hence, the initial proliferative KA bulb (Supporting Information: Figure S2E) exhibited supra-basal 14-3-3 $\sigma$ /K1 expression associated with weak p53/p21 (Figure 2C<sup>28</sup>); whereas overt KAs exhibited uniform 14-3-3 $\sigma$ /p53/p21, accompanied by premature basal-layer K1 expression in keratotic frond histotypes (Figure 2C).<sup>28</sup> These links between 14-3-3 $\sigma$  and *fos*/*PTEN* which triggered p53/p21, may also account for basal-to-supra-basal changes in p-AKT<sup>ser473</sup> expression,<sup>28</sup> where differentiation to inhibit AKT and/or restrict expression to supra-basal layers (Figure 6)<sup>30-32,41</sup> contributed to a KA outcome rather than malignant progression.

Additional *ras<sup>Ha</sup>* activation in *HK1.ras/fos- $\Delta$ 5PTEN<sup>flx/flx</sup>* mice altered papillomatogenesis, giving rise to tumors that converted to malignancy, which centered on 14-3-3 $\sigma$  interactions with MDM2 leading to p53 loss.<sup>3,4,22</sup> Here, tri-genic *HK1.ras/fos- $\Delta$ 5PTEN<sup>flx/flx</sup>* mice also identified 14-3-3 $\sigma$  interactions with p21, that appeared to limit early-stage malignant progression via AKT inhibition. Initially, in normal epidermis and preneoplastic *HK1.ras* or *HK1.ras/fos* hyperplasia, activated p-MDM2<sup>166</sup> expression was supra-basal alongside 14-3-3 $\sigma$ , and in basal-layers, sporadic p-MDM2<sup>166</sup> was also associated with p53/p21 co-expression in keratinocytes completing the cell cycle (Figure 1A,B).<sup>3,4,22,38</sup> Such supra-basal 14-3-3 $\sigma$ /p-MDM2<sup>166</sup> may be a feature of epidermal homeostasis where p-MDM2<sup>166</sup>-mediated removal of p53, alongside supra-basal AKT activation, facilitates terminal differentiation to prevent deregulated apoptosis and maintain barrier functions.<sup>28,41</sup> Indeed, this aspect of barrier homeostasis<sup>17-19,42</sup> may underlie the minimal p53/p21 responses

observed in *HK1.ras/fos* hyperplasia; possibly reflecting an epidermal tolerance to such *ras/fos*-mediated proliferation (Figure 1A,B).<sup>27-29</sup>

In overt *HK1.ras*, *HK1.ras/fos* and *HK1.ras- $\Delta$ 5PTEN<sup>flx/flx</sup>* papillomas, this supra-basal 14-3-3 $\sigma$ /p-MDM2<sup>166</sup> profile continued yet increasing 14-3-3 $\sigma$  appeared in strands of basal papilloma keratinocytes and was accompanied by strong, uniform nuclear p53 expression. As 14-3-3 $\sigma$  is a chaperone that removes MDM2 from the nucleus for ubiquitination, increased 14-3-3 $\sigma$  expression led to elevated, nuclear p53<sup>3,4,22</sup> that subsequently inhibited malignant conversion; a feature of these bi-genic mice.<sup>26-29</sup> This was consistent with rapid papillomatogenesis observed in 14-3-3 $\sigma$  knockout mice following two-stage chemical carcinogenesis<sup>26</sup> and susceptibility to skin carcinogenesis in repeated epilation mice (*Er/Er*) that express a truncated 14-3-3 $\sigma$  protein.<sup>23,24</sup>

In tri-genic *HK1.ras/fos- $\Delta$ 5PTEN<sup>flx/flx</sup>* hyperplasia and papillomas, elevated 14-3-3 $\sigma$ , p53 and p21 expression responses were immediate, appearing in all layers; and with a noted diminished 14-3-3 $\sigma$ /p21 co-expression in the acanthotic regions (Figure 3A,6A) suggesting direct 14-3-3 $\sigma$ /p21 interactions (see below). Such 14-3-3 $\sigma$ /p53/p21 responses helped maintained supra-basal p-MDM2<sup>166</sup> expression (Figure 5B,C) together with AKT inhibition (Figure 6A); thus, despite significant increased hyperplasia and rapid papilloma formation, malignant conversion was delayed, for example, in contrast to TPA promotion (below). However, with time basal-layer 14-3-3 $\sigma$  expression decreased (Figure 3C: wdSCC1 and 2), and this was paralleled by supra-basal-to-basal increases in activated p-MDM2<sup>166</sup> (Figure 5C), resulting in p53 down regulation and increased spontaneous mutations in proliferative basal cells resulting in conversion to wdSCCs.<sup>29</sup>

Of note, this wdSCC histotype was maintained over the medium term and thus mimics persistent p53-independent, 14-3-3 $\sigma$  expression observed in many human tumors.<sup>11-16</sup> Indeed, this remained the case until 14-3-3 $\sigma$  expression was lost during progression to more aggressive SCC (Figures 5C and 6C). Here, despite reduced 14-3-3 $\sigma$  in wdSCC basal layer cells, supra-basal expression continued, probably trans-activated by p63 (primarily TAp63 $\gamma$ ) in the absence of p53.<sup>43</sup> This supports the idea that 14-3-3 $\sigma$  roles in differentiation (above<sup>18,19</sup>; also contribute to maintenance of wdSCC histotypes, such as maintaining persistent (albeit reduced) keratin K1 expression; as keratin K1 (or K10) expression inhibits transformation<sup>44,45</sup> and were rapidly lost in TPA promotion experiments (Figure 4). In addition, 14-3-3 $\sigma$ /p21 interactions<sup>32,46</sup> may also inhibit AKT activity to limit early-stage malignant progression (below<sup>30,31,47</sup>). Nonetheless, persistent 14-3-3 $\sigma$  in p53-negative wdSCCs cannot exclude oncogenic roles, as suggested in vitro by malignant T52 carcinoma cells (below); that is, in cells lacking p53, once protection failed, spontaneous mutations increased with potential to cooperate with persistent, deregulated 14-3-3 $\sigma$  expression and dictate the outcome as observed in human tumor progression and patient prognosis.<sup>8,15,16</sup>

In terms of *HK1.ras/fos- $\Delta$ 5PTEN<sup>flx/flx</sup>* progression, previous studies showed that p53-independent p21 expression limited malignant progression,<sup>29,46</sup> and as 14-3-3 $\sigma$ /p21 co-expression in hyperplasia/papilloma varied with the degree of acanthosis

(Figures 3A and 6A) this strengthens their direct interactions.<sup>32,38</sup> Moreover, 14-3-3 $\sigma$  and p21 are known inhibitors of AKT,<sup>31–33,46,47</sup> which maybe a key activity that limited early-stage malignant progression following p53 loss. Previously, western blot analysis of TPA-promoted *HK1.ras- $\Delta$ PTEN<sup>flx/flx</sup>* mice showed immediate increases in p-AKT expression in hyperplasia and papillomas, culminating in strong expression in aggressive SCC.<sup>27</sup> Subsequently, p-AKT inhibition appeared to be a direct target of compensatory p53/p21 expression in *HK1.fos- $\Delta$ PTEN<sup>flx/flx</sup>* mice<sup>28</sup> and, as shown in *HK1.ras/fos- $\Delta$ PTEN<sup>flx/flx</sup>* mice following p53 loss,<sup>29</sup> persistent p21 was again associated with low-level p-AKT1<sup>ser473</sup>; now appearing alongside 14-3-3 $\sigma$  expression (Figure 6).

Thus, given the levels of 14-3-3 $\sigma$ /p21 observed during *HK1.ras/fos- $\Delta$ PTEN<sup>flx/flx</sup>* papillomatogenesis (Figure 6A), their combined co-expression (alongside that of p53; Figures 1–3), may help account for the distinct lack of p-AKT1<sup>ser473</sup> despite PTEN ablation. This lack had been an intriguing result, given loss of PTEN-mediated AKT signaling regulation had been expected to result in elevated p-AKT1<sup>473</sup> expression.<sup>27–29</sup> Further, it may be that such persistent basal-layer 14-3-3 $\sigma$ /p21 still restricted the increasing levels of p-AKT1<sup>473</sup> expression to supra-basal layers of early *HK1.ras/fos- $\Delta$ PTEN<sup>flx/flx</sup>* wdSCCs (Figure 6B). However, with time, beginning with 14-3-3 $\sigma$ , both 14-3-3 $\sigma$  and p21 expression faded and increased, uniform basal-layer p-AKT<sup>ser473</sup> expression was associated with progression to aggressive SCC, presumably combined with increasing spontaneous mutations given the lack of p53 surveillance.

Furthermore, the protective nature of this 14-3-3 $\sigma$ /p21/p53 TSG triad was clearly demonstrated by rapid progression to pdSCCs following TPA promotion of *HK1.ras- $\Delta$ PTEN<sup>flx/flx</sup>* mice.<sup>27</sup> Here, *HK1.ras- $\Delta$ PTEN<sup>flx/flx</sup>* pdSCCs were devoid of 14-3-3 $\sigma$  and K1 (Figure 4A,B; Supporting Information: Figure S5); and deployment of protective 14-3-3 $\sigma$ /p53/p21 expression was short lived, as analysis of TPA-promoted *HK1.ras- $\Delta$ PTEN<sup>flx/flx</sup>* papillomas and the earliest hyperplasia, were already negative for 14-3-3 $\sigma$ /p53/p21 expression (Figure 4). Thus, TPA-promoted *HK1.ras- $\Delta$ PTEN<sup>flx/flx</sup>* papillomatogenesis was rapid, as also observed in two-stage chemical carcinogenesis employing 14-3-3 $\sigma$  knockouts<sup>26</sup>; with uniform p-AKT1<sup>ser473</sup> helping drive early papillomatogenesis, consistent with previous western blot analysis<sup>27</sup> with rapid malignant conversion and progression to pdSCC (Figure 6). These data suggest important roles for AKT activation in malignant progression and, together with that of p-mTOR, are under further investigation in 14-3-3 $\sigma$  and p21 knockout models to confirm the significance and causality of stage-specific 14-3-3 $\sigma$  and/or p21 loss and subsequent AKT/p-mTOR overexpression.

In vitro, membranous 14-3-3 $\sigma$  expression profiles observed in proliferative HaCaT and benign SP1 papilloma cells were consistent with suppressive roles<sup>5,17–19,42</sup>; while the distinct cytoplasmic polarity of 14-3-3 $\sigma$  expression in SP1<sup>ras61</sup> papilloma keratinocytes again suggested a degree of spatial awareness<sup>5,19,42</sup>; as seen in *HK1.fos- $\Delta$ PTEN<sup>flx/flx</sup>* hyperplasia (Figure 2B). Unexpectedly in 2D cultures, malignant T52<sup>ras61/HVVfos</sup> SCC cells retained membranous 14-3-3 $\sigma$  and cytoplasmic polarity, despite their resistance to terminal

differentiation.<sup>33</sup> This raised oncogenic implications for persistent (or secreted) 14-3-3 $\sigma$  expression<sup>11–14</sup> that may contribute to cellular migration during early invasion, as observed in mammary carcinogenesis<sup>40</sup>; however, in 3D cultures, 14-3-3 $\sigma$  expression was sporadic and was lost in individual invading T52<sup>ras61/HVVfos</sup> SCC cells (Figure 7).

This alternate view of potential oncogenic roles regarding persistent, p53-independent 14-3-3 $\sigma$  expression likely reflect the multitude of interactions assigned to 14-3-3 $\sigma$  activities and are clearly context dependent.<sup>1,2,7</sup> For instance, while elevated 14-3-3 $\sigma$  counters ras<sup>Ha</sup><sup>26</sup> and fos activation,<sup>33</sup> and alongside p21, responds to loss of PTEN-mediated AKT regulation,<sup>26–32,46,47</sup> the roles for 14-3-3 $\sigma$  in cell rigidity and migration observed in mammary carcinogenesis<sup>40</sup> may interact with the loss of PTEN functions in cell spreading and migration.<sup>48,49</sup> Further, during wound healing, 14-3-3 $\sigma$  is known to stimulate the PI3K/mTOR pathway increasing cell growth and migration.<sup>36,50</sup> Here, alternate keratins are expressed such as K17,<sup>51</sup> that aid keratinocyte migration via direct cytoplasmic interactions with 14-3-3 $\sigma$  to stimulate mTOR activities.<sup>50,51</sup> This fits in well with largely subcellular cytoplasmic location of 14-3-3 $\sigma$  in the tumor cell lines and potentially invasion roles in graft assays<sup>35,40</sup> together with the membranous expression and changes in cell shape as keratinocytes committed to differentiate.

Finally, in p53-positive tumors,<sup>9–16</sup> the oncogenic contribution of persistent 14-3-3 $\sigma$  expression maybe indirect, for example, reduced MDM2 leading to elevated expression of (UVB-mediated) gain-of-function p53 mutants.<sup>21</sup>

Taken collectively, in vivo data highlight 14-3-3 $\sigma$  suppressive roles geared to limit ras<sup>Ha</sup>-activated papillomatogenesis via increased p53<sup>26,27</sup> or exploit differentiation roles as in KA etiology that link 14-3-3 $\sigma$  to fos and PTEN. On tumor progression, decreased 14-3-3 $\sigma$  and increased p-MDM2<sup>166</sup> activity reduced p53 leading to malignant conversion; yet 14-3-3 $\sigma$ /p21 co-expression continued to limit early-stage malignant progression via p-AKT<sup>473</sup> inhibition; until circumvented as observed in TPA promotion experiments. Given the diverse, context-dependent nature of 14-3-3 $\sigma$  activities in human tumors, multistage transgenic models are likely to help validate the tumor suppressive or potentially oncogenic roles for 14-3-3 $\sigma$  deregulation.

## AUTHOR CONTRIBUTIONS

*The conception and design of the study:* David A. Greenhalgh. *Wrote the manuscript:* David A. Greenhalgh. *Critiqued the output for important intellectual content:* David A. Greenhalgh. *The organization of the conduct of the study:* David A. Greenhalgh, Carol M. McMenemy, and Jean A.Quinn. *Carrying out the study:* David A. Greenhalgh, Carol M. McMenemy, Dajiang Guo, and Jean A.Quinn. *The analysis and interpretation of study data:* David A. Greenhalgh, Carol M. McMenemy, Dajiang Guo, and Jean A.Quinn.

## ACKNOWLEDGMENTS

We would like to thank Ashley Cochrane, Scott Joel Heng, Justine Frazer, Karen Crookston, and Jamie Boyle for their assistance with immunofluorescence/IHC analysis and tissue culture during their

short-term research projects. We also thank Mary Doherty, Stuart Lannigan, and Craig Begley for assistance with animal husbandry. This work was supported in part by the Scott Endowment Fund for Dermatology (C. M. M.; D. G.); funds from the GU M.Res Research Program in Cancer Sciences (C. M. M.; D. G.; KC; JB); the SFC/MRC M.Res in Integrative Mammalian Biology, Glasgow University (AC), and a Wellcome Biomedical vacation scholarship (SJH) (UNS22162).

### CONFLICT OF INTEREST STATEMENT

The authors declare no conflict of interest.

### DATA AVAILABILITY STATEMENT

The data that support the findings of this study are available from the corresponding author upon reasonable request and are also deposited in Enlighten Database Glasgow University. <https://www.gla.ac.uk/myglasgow/openaccess/Greenhalgh> For the purpose of open access, the author(s) has applied a Creative Commons Attribution (CC BY) licence to any Author Accepted Manuscript version arising from this submission.

### ORCID

David A. Greenhalgh  <http://orcid.org/0000-0002-6737-2744>

### REFERENCES

- Pennington KL, Chan TY, Torres MP, Andersen JL. The dynamic and stress-adaptive signaling hub of 14-3-3: emerging mechanisms of regulation and context-dependent protein-protein interactions. *Oncogene*. 2018;37:5587-5604.
- Aghazadeh Y, Papadopoulos V. The role of the 14-3-3 protein family in health, disease, and drug development. *Drug Discov Today*. 2016;21:278-287.
- Hermeking H, Benzinger A. 14-3-3 proteins in cell cycle regulation. *Sem Cancer Biol*. 2006;16:183-192.
- Hermeking H, Lengauer C, Polyak K, et al. Is a p53-regulated inhibitor of G2/M progression. *Mol Cell*. 1997;1:3-11.
- Ling C, Zuo D, Xue B, Muthuswamy S, Muller WJ. A novel role for 14-3-3 $\sigma$  in regulating epithelial cell polarity. *Genes Dev*. 2010;24:947-956.
- Lodygin D, Hermeking H. The role of epigenetic inactivation of 14-3-3 $\sigma$  in human cancer. *Cell Res*. 2005;15:237-246.
- Phan L, Chou PC, Velazquez-Torres G, et al. The cell cycle regulator 14-3-3 $\sigma$  opposes and reverses cancer metabolic reprogramming. *Nat Commun*. 2015;6:7530.
- Ko S, Kim JY, Jeong J, Lee JE, Yang WI, Jung WH. The role and regulatory mechanism of 14-3-3 sigma in human breast cancer. *J Breast Cancer*. 2014;17:207-218.
- Iwata N, Yamamoto H, Sasaki S, et al. Frequent hypermethylation of CpG islands and loss of expression of the 14-3-3 $\sigma$  gene in human hepatocellular carcinoma. *Oncogene*. 2000;19:5298-5302.
- Yatabe Y, Osada H, Tatematsu Y, Mitsudomi T, Takahashi T. Decreased expression of 14-3-3 $\sigma$  in neuroendocrine tumors is independent of origin and malignant potential. *Oncogene*. 2002;21:8310-8319.
- Shiba-Ishii A, Noguchi M. Aberrant stratifin overexpression is regulated by tumor-associated CpG demethylation in lung adenocarcinoma. *Am J Pathol*. 2012;180:1653-1662.
- Radhakrishnan VM, Jensen TJ, Cui H, Futscher BW, Martinez JD. Hypomethylation of the 14-3-3 $\sigma$  promoter leads to increased expression in non-small cell lung cancer. *Genes Chromosomes Cancer*. 2011;50:830-836.
- Perathoner A, Pirkebner D, Brandacher G, et al. 14-3-3 $\sigma$  expression is an independent prognostic parameter for poor survival in colorectal carcinoma patients. *Clin Cancer Res*. 2005;11:3274-3279.
- Liu CC, Chang TC, Lin YT, et al. Paracrine regulation of matrix metalloproteinases contributes to cancer cell invasion by hepatocellular carcinoma-secreted 14-3-3 $\sigma$ . *Oncotarget*. 2016;7:36988-36999.
- Tanaka K, Hatada T, Kobayashi M, et al. The clinical implication of 14-3-3 sigma expression in primary gastrointestinal malignancy. *Int J Oncol*. 2004;25:1591-1597.
- Winter M, Rokavec M, Hermeking H. 14-3-3 $\sigma$  Functions as an intestinal tumor suppressor. *Cancer Res*. 2021;81:3621-3634.
- Hammond NL, Headon DJ, Dixon MJ. The cell cycle regulator protein 14-3-3 $\sigma$  is essential for hair follicle integrity and epidermal homeostasis. *J Invest Dermatol*. 2012;132:1543-1553.
- Sun BK, Boxer LD, Ransohoff JD, et al. CALML5 is a ZNF750- and TINC2-induced protein that binds stratifin to regulate epidermal differentiation. *Genes Dev*. 2015;29:2225-2230.
- Sambandam SAT, Kasetti RB, Xue L, Dean DC, Lu Q, Li Q. 14-3-3 $\sigma$  regulates keratinocyte proliferation and differentiation by modulating Yap1 cellular localization. *J Invest Dermatol*. 2015;135:1621-1628.
- Lodygin D, Yazdi AS, Sander CA, Herzinger T, Hermeking H. Analysis of 14-3-3 $\sigma$  expression in hyperproliferative skin diseases reveals selective loss associated with CpG-methylation in basal cell carcinoma. *Oncogene*. 2003;22:5519-5524.
- Caulin C, Nguyen T, Lang GA, et al. An inducible mouse model for skin cancer reveals distinct roles for gain- and loss-of-function p53 mutations. *J Clin Invest*. 2007;117:1893-1901.
- Lee MH, Lozano G. Regulation of the p53-MDM2 pathway by 14-3-3 $\sigma$  and other proteins. *Sem Cancer Biol*. 2006;16:225-234.
- Herron BJ, Liddell RA, Parker A, et al. A mutation in stratifin is responsible for the repeated epilation (Er) phenotype in mice. *Nat Genet*. 2005;37:1210-1212.
- Lutzner MA, Guenet JL, Breitburd F. Multiple cutaneous papillomas and carcinomas that develop spontaneously in a mouse mutant, the repeated epilation heterozygote Er/+. *J Natl Cancer Inst*. 1985;75:161-166.
- Ling C, Su VMT, Zuo D, Muller WJ. Loss of the 14-3-3 $\sigma$  tumor suppressor is a critical event in ErbB2-mediated tumor progression. *Cancer Discov*. 2012;2:68-81.
- Winter M, Lodygin D, Verdoodt B, Hermeking H. Deletion of 14-3-3 $\sigma$  sensitizes mice to DMBA/TPA-induced papillomatosis. *Oncotarget*. 2016;7:46862-46870.
- Yao D, Alexander CL, Quinn JA, Porter MJ, Wu H, Greenhalgh DA. PTEN loss promotes rasHa-mediated papillomatogenesis via dual up-regulation of AKT activity and cell cycle deregulation but malignant conversion proceeds via PTEN-associated pathways. *Cancer Res*. 2006;66:1302-1312.
- Yao D, Alexander CL, Quinn JA, Chan WC, Wu H, Greenhalgh DA. Fos cooperation with PTEN loss elicits keratoacanthoma not carcinoma, owing to p53/p21WAF-induced differentiation triggered by GSK3 $\beta$  inactivation and reduced AKT activity. *J Cell Sci*. 2008;121:1758-1769.
- Macdonald FH, Yao D, Quinn JA, Greenhalgh DA. PTEN ablation in Ras(Ha)/Fos skin carcinogenesis invokes p53-dependent p21 to delay conversion while p53-independent p21 limits progression via cyclin D1/E2 inhibition. *Oncogene*. 2014;33:4132-4143.
- Yang H, Wen Y-Y, Zhao R, et al. DNA damage-induced protein 14-3-3 $\sigma$  inhibits protein kinase B/Akt activation and suppresses Akt-activated cancer. *Cancer Res*. 2006;66:3096-3105.
- Shao Z, Cai Y, Xu L, et al. Loss of the 14-3-3 $\sigma$  is essential for LASP1-mediated colorectal cancer progression via activating PI3K/AKT signaling pathway. *Sci Rep*. 2016;6:25631.

32. Hemmati PG, Normand G, Gillissen B, Wendt J, Dörken B, Daniel PT. Cooperative effect of p21Cip1/WAF-1 and 14-3-3 $\sigma$  on cell cycle arrest and apoptosis induction by p14ARF. *Oncogene*. 2008;27:6707-6719.
33. Greenhalgh DA, Quintanilla MI, Orengo CC, et al. Cooperation between v-fos and v-ras<sup>H</sup>a induces autonomous papillomas in transgenic epidermis but not malignant conversion. *Cancer Res*. 1993;53:5071-5075.
34. Berton TR, Wang XJ, Zhou Z, et al. Characterization of an inducible, epidermal-specific knockout system: differential expression of lacZ in different Cre reporter mouse strains. *Genesis*. 2000;26:160-161.
35. Greenhalgh DA, Yuspa SH. Malignant conversion of murine squamous papilloma cell lines by transfection with the fos oncogene. *Mol Carcinog*. 1988;1:134-143.
36. Edward M, Quinn JA, Sands W. Keratinocytes stimulate fibroblast hyaluronan synthesis through the release of stratifin: a possible role in the suppression of scar tissue formation. *Wound Repair Regen*. 2011;19:379-386.
37. Henseleit U, Zhang J, Wanner R, Haase I, Kolde G, Rosenbach T. Role of p53 in UVB-induced apoptosis in human HaCaT keratinocytes. *J Invest Dermatol*. 1997;109:722-727.
38. Laronga C, Yang HY, Neal C, Lee MH. Association of the cyclin-dependent kinases and 14-3-3 sigma negatively regulates cell cycle progression. *J Biol Chem*. 2000;275:23106-23112.
39. Cianfarani F, Bernardini S, De Luca N, et al. Impaired keratinocyte proliferative and clonogenic potential in transgenic mice overexpressing 14-3-3 $\sigma$  in the epidermis. *J Invest Dermatol*. 2011;131:1821-1829.
40. Boudreau A, Tanner K, Wang D, Geyer FC, Reis-Filho JS, Bissell MJ. 14-3-3 $\sigma$  stabilizes a complex of soluble actin and intermediate filament to enable breast tumor invasion. *Proc Natl Acad Sci*. 2013;110:E3937-E3944.
41. Calautti E, Li J, Saoncella S, Brissette JL, Goetinck PF. Phosphoinositide 3-kinase signaling to Akt promotes keratinocyte differentiation versus death. *J Biol Chem*. 2005;280:32856-32865.
42. Dellambra E, Golisano O, Bondanza S, et al. Downregulation of 14-3-3 $\sigma$  prevents clonal evolution and leads to immortalization of primary human keratinocytes. *J Cell Biol*. 2000;149:1117-1130.
43. Trink B, Osada M, Ratovitski EA, Sidransky D. p63 transcriptional regulation of epithelial integrity and cancer. *Cell Cycle*. 2007;6:240-245.
44. Kartasova T, Roop DR, Yuspa SH. Relationship between the expression of differentiation-specific keratins 1 and 10 and cell proliferation in epidermal tumors. *Mol Carcinog*. 1992;6:18-25.
45. Santos M, Paramio JM, Bravo A, Ramirez A, Jorcano JL. The expression of keratin K10 in the basal layer of the epidermis inhibits cell proliferation and prevents skin tumorigenesis. *J Biol Chem*. 2002;277:19122-19130.
46. Topley GI, Okuyama R, Gonzales JG, Conti C, Dotto GP. p21(WAF1/Cip1) functions as a suppressor of malignant skin tumor formation and a determinant of keratinocyte stem-cell potential. *Proc Natl Acad Sci*. 1999;96:9089-9094.
47. Zhou BP, Liao Y, Xia W, Spohn B, Lee MH, Hung MC. Cytoplasmic localization of p21Cip1/WAF1 by Akt-induced phosphorylation in HER-2/neu-overexpressing cells. *Nat Cell Biol*. 2001;3:245-252.
48. Kotelevets L, Hengel J, Bruyneel E, Mareel M, Roy F, Chastre E. Implication of the MAGI-1b/PTEN signalosome in stabilization of adherens junctions and suppression of invasiveness. *FASEB J*. 2005;19:115-117.
49. Subauste MC, Nalbant P, Adamson ED, Hahn KM. Vinculin controls PTEN protein level by maintaining the interaction of the adherens junction protein  $\beta$ -catenin with the scaffolding protein MAGI-2. *J Biol Chem*. 2005;280:5676-5681.
50. Kim S, Wong P, Coulombe PA. A keratin cytoskeletal protein regulates protein synthesis and epithelial cell growth. *Nature*. 2006;441:362-365.
51. Mikami T, Maruyama S, Abé T, et al. Keratin 17 is co-expressed with 14-3-3 sigma in oral carcinoma in situ and squamous cell carcinoma and modulates cell proliferation and size but not cell migration. *Virchows Arch*. 2015;466:559-569.

#### SUPPORTING INFORMATION

Additional supporting information can be found online in the Supporting Information section at the end of this article.

**How to cite this article:** McMenemy CM, Guo D, Quinn JA, Greenhalgh DA. 14-3-3 $\sigma$ /Stratifin and p21 limit AKT-related malignant progression in skin carcinogenesis following MDM2-associated p53 loss. *Mol Carcinogen*. 2024;63:1768-1782. doi:10.1002/mc.23771